Alma Mater Studiorum · University of Bologna

School of Science
Department of Physics and Astronomy
Master Degree in Physics

Love number for Quantum Black Holes

Supervisor:
Prof. Roberto Casadio

Submitted by:
Alex-Cristian Cozma

Academic Year 2022/2023

Abstract

This thesis aims at providing a computation of the "electrical" quadrupolar Love number for a quantum black hole by using the hydrogen model for its energy spectrum. The "electrical" quadrupolar Love number is a quantity that carries informations on the physical deformation of a body under tidal forces, in the case of quantum black holes, it carries information about the interior of the black hole, it is therefore considered important since it might be a good target for measurement by future gravitational experiments such as LISA.

Contents

Chapter 1

Black holes in General Relativity

The discovery of the theory of general relativity by Albert Einstein led to various interesting theoretical concepts and predictions that turned out to be observed in nature, one of the notoriously most fascinating objects predicted by the theory is the "black hole", in this chapter we will make a short review of tools of general relativity that are necessary to theorize the existence of black holes from a purely a mathematical perspective. The following introduction to General Relativity and black holes is based on [2, 3, 1]

1.1 Einstein's field equations

Einstein's field equations are the main result of the General Relativity theory, they provide a mathematical description of gravity as a result of space-time being curved by matter and energy. To understand these equations we begin with the fundamental concept of the metric tensor, denoted as $g_{\mu\nu}$. This tensor describes the infinitesimal distances in space-time, as represented by the line element equation

$$ds^2 = g_{\mu\nu} dx^\mu dx^\nu. \tag{1.1}$$

It provides information on the curvature of space-time, that is how the distance between two events changes in different regions of space-time, that is, the $g_{\mu\nu}$ encodes informations about the curvature of a surface. In curved space-time, the paths of particles and light beams are described by geodesics, the geodesic equation, which determines the shortest path between two points in this curved space-time, is given by

$$\frac{d^2x^\lambda}{d\tau^2} + \Gamma^\lambda_{\mu\nu} \frac{dx^\mu}{d\tau} \frac{dx^\nu}{d\tau} = 0. \tag{1.2}$$

Here, $\Gamma^\lambda_{\mu\nu}$ are the Christoffel symbols or the affine connection, which relate the metric tensor to the derivatives of the metric, the affine connection is expressed as

$$\Gamma^\lambda_{\mu\nu} = \frac{1}{2} g^{\lambda\sigma} \left(\frac{\partial g_{\sigma\mu}}{\partial x^\nu} + \frac{\partial g_{\sigma\nu}}{\partial x^\mu} - \frac{\partial g_{\mu\nu}}{\partial x^\sigma} \right). \tag{1.3}$$

The curvature of spacetime is described by the Riemann curvature tensor as

$$R^{\lambda}_{\mu\nu\sigma} = \frac{\partial \Gamma^{\lambda}_{\mu\nu}}{\partial x^{\sigma}} - \frac{\partial \Gamma^{\lambda}_{\mu\sigma}}{\partial x^{\nu}} + \Gamma^{\rho}_{\mu\nu}\Gamma^{\lambda}_{\sigma\rho} - \Gamma^{\rho}_{\mu\sigma}\Gamma^{\lambda}_{\nu\rho}. \tag{1.4}$$

The Ricci tensor, a contracted form of the Riemann tensor, is given by

$$R_{\mu\sigma} = R^{\nu}_{\mu\nu\sigma}, \tag{1.5}$$

and the Ricci scalar, the trace of the Ricci tensor, is written as

$$R = g^{\mu\nu} R_{\mu\nu}. \tag{1.6}$$

Finally, Einstein's field equations, which are the ultimate result of General Relativity, link the geometry of spacetime to the distribution of matter and energy in it. They are expressed without the cosmological constant as

$$G_{\mu\nu} = 8\pi G T_{\mu\nu}, \tag{1.7}$$

where $G_{\mu\nu} = R_{\mu\nu} - \frac{1}{2} g_{\mu\nu} R$ is the Einstein tensor, and $T_{\mu\nu}$ is the stress-energy tensor. These equations encapsulate the essence of General Relativity and provide a mathematical description on how matter and energy influence the curvature of spacetime.

1.2 Black hole solutions

Einstein's field equations have several important solutions, each corresponding to different physical scenarios in the context of black holes and celestial bodies. Here, we list three key solutions: the Schwarzschild metric, the Reissner-Nordström metric, and the Kerr metric.

The Schwarzschild Metric

The Schwarzschild metric is the solution to Einstein's Field Equations that describes the gravitational field outside a spherical, non-rotating, and uncharged mass. It is given by the equation:

$$ds^2 = \left(1 - \frac{2m}{r}\right) dt^2 - \left(1 - \frac{2m}{r}\right)^{-1} dr^2 - r^2 \left(d\theta^2 + \sin^2\theta d\varphi^2\right) \tag{1.8}$$

where $d\Omega^2$ represents the angular part of the metric. This metric has a singularity at $r = 0$ and an event horizon at $r = 2m$

The Reissner-Nordström Metric

The Reissner-Nordström metric extends the Schwarzschild solution to include a charged, non-rotating spherical mass. It is expressed as:

$$ds^2 = \left(1 - \frac{2m}{r} - \frac{Q^2}{r^2}\right) dt^2 - \left(1 - \frac{2m}{r} - \frac{Q^2}{r^2}\right)^{-1} dr^2 + r^2 d\Omega^2, \tag{1.9}$$

where Q is the electric charge of the mass. This metric features two horizons and a singularity at the center.

The Kerr Metric

The Kerr metric describes the spacetime around a rotating mass. It is an axisymmetric solution to Einstein's field equations and is given by:

$$ds^2 = \left(1 - \frac{2mr}{\rho^2}\right) dt^2 - \frac{\rho^2}{\Delta} dr^2 - \rho^2 d\theta^2 + \left(r^2 + a^2 + \frac{2mra^2 \sin^2\theta}{\rho^2}\right) \sin^2\theta d\phi^2 + \frac{4mra \sin^2\theta}{\rho^2} d\phi dt, \tag{1.10}$$

where $\rho^2 = r^2 + a^2 \cos^2\theta$, $\Delta = r^2 - 2mr + a^2$, and a is the angular momentum per unit mass. The Kerr metric features an event horizon, an ergosphere, and a ring singularity.

Motivation for this work

In the framework of general relativity, black holes are described as entities featuring singularities, which represent mathematical anomalies indicative of the theory's limitations. These singularities, characterized by infinite quantities, reveal a fundamental inadequacy within general relativity, as it falls short of accurately depicting phenomena at quantum scales and under conditions of extreme energy—conditions, this highlights the essential need for integrating quantum mechanics into our understanding of black holes. Quantum mechanics, with its robust predictive power at small scales and high energies, offers a complementary perspective that, when combined with general relativity, could significantly enhance our comprehension of black hole interiors and potentially resolve the paradox of singularities marked by infinite quantities.

The pursuit of a unified theory that seamlessly blends general relativity (GR) and quantum mechanics (QM) for the exploration of black holes does not necessarily demand a fully developed framework, instead, as done in this thesis, perturbative methods may suffice in bridging the gap between these two pillars of physics, enabling progress in predictive accuracy and the study of black hole dynamics.

Empirical evidence plays a crucial role in testing theoretical predictions about the nature of black holes, observations, particularly of black hole mergers, are invaluable. These cosmic events, characterized by the interaction of tidal forces as black holes exert gravitational influence upon one another, offer profound insights into the structure and behavior of these enigmatic objects. In this context, Love numbers quantifiers of how a body's shape deforms in response to tidal forces emerge as critical tools for investigating the internal mechanics of black holes, providing a window into their most elusive aspects. The reason Love numbers are interesting is because they identically vanish for black holes described by only general relativity, this doesnt happen when quantum mechanics is introduced perturbatively, on top of that, there is a link between the model used to describe the black hole interior and the value of the Love number, we will adopt a model inspired by the hydrogen energy spectrum and will compute the Love number, showing that it is indeed non zero.

Chapter 2

Classical Love number

In this chapter we will follow the work of Ram Brustein and Yotam Sherf in "Classical Love numbers for quantum black holes" [6] integrating in the first and second section informations from R. Brustein and A. J. M. Medved, "Quantum hair of black holes out of equilibrium" [7] and "No-hair theorem for Black Holes in Astrophysical Environments" [8] for giving a more broad perspective on the associated research on perturbed black holes and their proprieties, in particular the article on quantum hair out of equilibrium highlights the effect of these perturbations on Hawking radiation and the link between what an external observer sees and what might be hidden inside the horizon at the heart of the black hole, the paper on "No hair" on the other hand provides a general relativity proof that Love numbers vanish for perturbed classical black holes.

2.1 Perturbed black holes

In classical understanding, the horizon of a black hole (BH) is seen as entirely opaque, obscuring any knowledge about its interior. Using quantum theory in equilibrium state, the scenario remains largely unchanged, although Hawking radiation is emitted, its rate of emission is incredibly slow, and it is mostly thermal, conveying minimal information about the BH's internal quantum state. The research in [7] however, shows a noticeable difference when a quantum BH is perturbed, it is proposed that such a BH can produce 'supersized' Hawking radiation, far more intense than that produced in equilibrium leading to the emergence of a new type of quantum hair, allowing external observers to discern the state and composition of the BH interior. Interestingly, this new hair's frequency and amplitude can be understood without resorting to new physical principles, and it decays much slower than the Schwarzschild time scale. This phenomenon can be detected through gravitational waves (and potentially other wave types) emissions, especially after a BH experiences a significant energy surge, like during and right after a BH merger (such conditions are also relevant in the discussion about Love numbers,

since such events lead to potential physical deformation). The presence of this new hair is expected to be a universal feature of quantum BHs, independent of the model used, these findings therefore shed new light on the understanding of BH and what they might "hide" behind the horizon. Until recently, the traditional view of a black hole's interior was generally accepted but the introduction of the firewall argument highlighted a conflict between this classical view and the principles of quantum theory, leading to the emergence of several non-traditional models proposing different internal structures for black holes. Despite these developments, there is still no unanimous agreement in the scientific community on an accurate description of a black hole's interior. Some theories even suggest the black hole interior should be conceptually removed from observable space-time. In [10] is proposed that the black hole interior is composed of a dynamic assembly of highly excited, interacting, long, closed strings, similar to a 'ball of string' or a collapsed polymer .

The recent detection of gravitational waves (GWs) from black hole mergers has transformed what was once a purely theoretical debate about the laws of quantum gravity into a more concrete discussion, every new theory about the nature of black holes must now be tested against these observational data. In addition to gravitational waves, there's also the potential of collecting the necessary data from electromagnetic waves and/or neutrinos.

Implications of a proposed polymer model for the black hole interior suggests that gravitational wave observations could serve as a tool to differentiate this model from the classical black hole concept and other proposed models. In the polymer model of the black hole interior, fluid modes coexist with the standard spacetime modes of a black hole's exterior, this results in their spectrum being an additive component to the ringdown or quasinormal modes (QNMs) of a perturbed black hole, also, according to this model, the black hole's outer surface behaves similarly to a traditional black hole horizon under certain conditions but remains partially opaque otherwise. As implied before, a key aspect of this fluidlike description is the emergence of a new type of quantum hair, this quantum hair is distinguished by emissions at lower frequencies and longer damping times compared to the QNMs of a classical black hole, these characteristics are influenced by various factors, including the Schwarzschild radius and the speed of light, with the velocity of sound for the fluid mode being, of course, less than the speed of light. The polymer model's distinctive approach is attributed to the introduction of a new scale, the string scale, which which has implications for the most experimentally accessible class of modes within this model.

In the context of the polymer model's fluidlike description of the black hole interior, an intriguing question would be about how internal fluid modes might couple with emitted gravitational waves (GWs) or other types of waves as observed from an external perspective arises. Let's think about the problem: an external observer, while having the option to disregard any knowledge about the black hole's interior, is still required to explain all observed phenomena within the framework of general relativity (GR) accord-

ing to Stephen Hawking's assertion that all conceivable data about a 'hidden' surface, limited by an observer's information, are equally probable.

From this viewpoint, the black hole's interior is primarily considered a theoretical construct used to elucidate its radiation emissions, the underlying assumption is that the black hole's horizon acts as a barrier, distinguishing these emissions from what an external observer can see. The focus is to demonstrate that external observers are likely to interpret any disturbances in the fluid modes of the black hole as external spacetime disturbances, rather than attributing them to the black hole's interior. This approach is crucial for connecting theoretical models of the black hole's internal workings with observable data from the outside.

Understanding the differing views on black holes requires recognizing that the external interpretation of fluid modes is as enigmatic as Hawking radiation itself, while various theories connect Hawking radiation to processes like pair production and quantum tunneling, insights into the black hole's interior can only come from external, indirect observations. Any theory explaining the Hawking effect is considered valid if it matches what we know or might discover about black holes. There is surely an advantage in thinking that Hawking radiation originates outside the black hole, this idea stems from the notion that this radiation, like all matter, cannot move through and emerge from the black hole's horizon.

The argument put forward is that from an external viewpoint, the fluid modes within black holes can be interpreted as "supersized" Hawking emissions, emissions that differ from standard emissions in that they represent large-amplitude coherent states involving photons, gravitons, and similar particles, on top of that, just as with standard Hawking radiation, these supersized modes are perceived to originate from the exterior spacetime of the black hole.

This interpretation holds true for both regular and supersized modes, maintaining consistency within the external perspective, the key factor here is the extent to which the black hole has diverged from its state of equilibrium. The degree of this deviation is directly influenced by the amount of energy injected into a specific mode, which in turn determines the amplitude of the emission, thus, the nature and intensity of these emissions are linked to the black hole's dynamic state. Supersized Hawking radiation emissions are rare because they require a significant energy input, usually absent in normal conditions, these large emissions are suppressed unless the black hole is significantly disturbed, on the contrary, the spontaneous particle production rate near a black hole's horizon in equilibrium can be theoretically predicted, resembling the Schwinger mechanism. This rate is highest for particles with energy levels typical of standard Hawking emissions.

Therefore, supersized Hawking radiation is an extremely rare event in undisturbed black holes, however, it could occur during the collision of two black holes in a binary system, where the significant energy released could trigger these large emissions. Gravitational waves from such mergers might be the most promising, or possibly the only,

way to observe supersized Hawking radiation.

Normally, black holes in equilibrium are known to have hair related to gauge fields and their conserved charges. It's a recognized fact that a perturbed black hole returns to equilibrium by losing this non-gauge-symmetry hair, typically in an exponential manner.

The key idea here is that black holes diverging from general relativity (GR) predictions may have a different timescale for shedding this hair. This timescale would differ from the familiar Schwarzschild or light-crossing times of black holes, even after shedding this specific type of hair, a black hole would largely maintain its classical GR characteristics, especially in aspects related to symmetry-associated hair.

External point of view

From the perspective of an external observer, only phenomena occurring on their side of the black hole's horizon are observable, this means that any form of radiation, be it conventional or supersized Hawking radiation, is perceived as originating from outside the horizon, When a black hole is near its equilibrium state, an external observer can employ a specific observational approach, known as the "horizon-locking gauge," to analyze the geometry near the horizon of the black hole, in this gauge, the equilibrium position of the black hole's outer surface, or its effective horizon, remains fixed at the Schwarzschild radius, even under considerable perturbations.

Understanding an external observer's perception of supersized quantum radiation from a black hole necessitates examining how the black hole deviates from its equilibrium state. A useful comparison can be drawn from classical physics, such as considering the deformation of the horizon of a slowly rotating black hole due to external tidal forces, this comparison aids in visualizing how significant alterations in a black hole's condition can produce noticeable effects, like the emission of supersized quantum radiation, from an external standpoint.

The concept of horizon deformation in black holes, pivotal for comprehending external views of supersized quantum radiation, was initially introduced by Hartle and later expanded by O'Sullivan and Hughes. Their method involves imagining this deformation by placing a distorted sphere in a three-dimensional, flat Euclidean space. The principal idea here is to keep the sphere's outer surface fixed and interpret its deformation in terms of changes in the associated Ricci curvature. Alternatively, this deformation can be perceived as the discrepancy between the location of the outer surface and the Schwarzschild radius (RS). In this context, the Schwarzschild radius represents the degree to which the internal fluid either protrudes from or withdraws into the fiducial horizon.

To assist in visualizing this concept, consider a black hole's horizon undergoing a static quadrupole deformation, this deformation changes the sphere's shape in a manner that scales with the strength of the perturbation, as described by the equation $P_2(\theta) = \frac{1}{2}(3\cos^2\theta - 1)$.

This equation represents the second Legendre polynomial in terms of the polar angle

θ. More generally, the position and shape of the deformed horizon are expected to oscillate over time, reflecting the dynamic interplay between the black hole's interior processes and how they are perceived by an observer outside the horizon.

Contrary to what might be expected, the deformed surface of a black hole can exhibit both indentations and bulges, regardless of the direction of the external force causing the perturbation, as depicted in certain illustrations (figure 2.1).

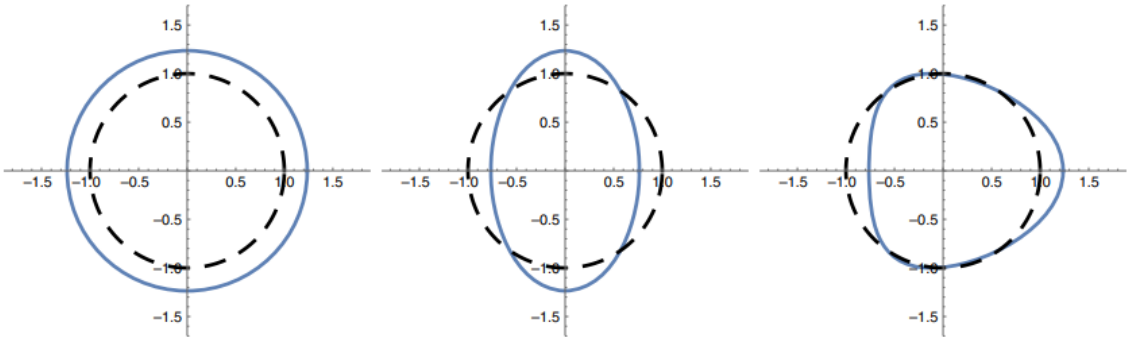

Figure 2.1: From [7] Visualization of a black hole's horizon undergoing a scalar, dipole and quadruple deformation respectively.

This analysis centers on areas where the black hole's horizon shows inward curvature or appears as if the internal matter of the black hole is protruding outward. This suggests that a part of the black hole's core may have been temporarily exposed to the external spacetime continuum. From the perspective of an observer outside the black hole, such an indentation in the horizon might be seen as the black hole absorbing negative energy. This viewpoint is consistent with the established theory that explains the emission of standard Hawking radiation.

However, the idea of a negative energy flow is mainly a theoretical tool for external observers. Its purpose is to uphold the principle of energy conservation in scenarios where positive energy is being emitted from the black hole. This concept, while theoretically significant, is primarily used to reconcile observations and theories regarding energy dynamics around black holes.

In the classical framework pertaining to tidal deformations of black holes' horizons, an emission of energy is generally linked exclusively with the superradiant modes inherent to a rotating black hole. Regarding the emission of Hawking radiation from a polymer black hole, both the emitted energy flux and its compensatory negative flux are ascribed internally to a quantum mechanical phenomenon, this phenomenon encompasses the disintegration of minuscule string loops from the black hole's interior, which is densely packed with strings. In the case of supersized Hawking radiation, it is hypothesized that the pattern would be analogous, albeit involving a considerable segment of the string

detaching in unison within a condensed timeframe.

From the internal perspective of the black hole, the relative deformation of the horizon, denoted as $\Delta L/L$, caused by a specific restoring force (considering, for instance, the Ith force), is expressed by the ratio:

$$\frac{\Delta L}{L_I} \sim \frac{(\Delta E)_I}{E} = \frac{p_I}{\rho} = \frac{v_I^2}{c^2} \tag{2.1}$$

In this equation, ΔL represents the change in the length scale of the horizon deformation, L_I is the characteristic length scale of the Ith force, $(\Delta E)_I$ is the energy change due to the Ith force, E is the total energy, p_I is the pressure associated with the Ith force, ρ is the density, v_I is the velocity, and c is the speed of light. This ratio quantifies the extent of the horizon's deformation in response to various forces and is a critical factor in understanding the internal dynamics of black holes. In this context, v_I represents the sound velocity for the Ith mode, p_I is its pressure, and $\rho \approx \frac{M_{BH}}{R_S^3}$ is the total energy density, where M_{BH} is the black hole mass. These relationships are derived using standard thermodynamic principles that link stress with strain and the ratio of pressure to energy density with sound velocity.

We can use Equation (2.1) to derive an expression for the redshift at the furthest extent of the protruding fluid:

$$\sqrt{-g_{tt}}\Big|_I = \sqrt{1 - \frac{R_S}{r_I}} = \sqrt{1 - \frac{R_S}{R_S(1 + \frac{\Delta L}{L}|_I)}} \approx \sqrt{\frac{\Delta L}{L}|_I}, \tag{2.2}$$

which implies that

$$\sqrt{-g_{tt}}\Big|_I \approx \frac{v_I}{c}. \tag{2.3}$$

These estimates are crucial for determining the mode frequencies as observed from outside the black hole and they help in verifying whether the observations made by an external observer are consistent with those from an internal perspective.

It is important to note that these equations are not compatible with a relativistic speed of sound $v_I = c$, in such a scenario, the ratio $\Delta L/L$ cannot be small, indicating that the limiting case of $v_I = c$ presents complications.

2.1.1 Hawking's radiation

The energy change associated with Hawking radiation, denoted as $(\Delta E)_H$, is approximately equal to the Hawking temperature T_H, which is inversely proportional to the Schwarzschild radius R_S. This relationship is expressed as:

$$(\Delta E)_H \sim T_H = \frac{1}{R_S}. \tag{2.4}$$

Considering the total energy E to be equivalent to the black hole mass M_{BH}, we have:

$$E = M_{BH}. \tag{2.5}$$

From this, it follows that the ratio of the energy change due to Hawking radiation to the total energy is:

$$\frac{(\Delta E)_H}{E} \sim \frac{1}{R_S M_{BH}} = \frac{1}{S_{BH}}, \tag{2.6}$$

where S_{BH} is the black hole entropy. The redshift at the location of the protruding fluid, which is also the perceived source location for an external observer, is given by:

$$\sqrt{-g_{tt}}\bigg|_H = \sqrt{\frac{1}{S_{BH}}} = \frac{l_P}{R_S}, \tag{2.7}$$

where the subscript H indicates a property associated with Hawking radiation (e.g., T_H is the Hawking temperature), and l_P is the Planck length.

This redshift value represents the location of the source of the radiation as perceived by an external observer. When it comes to the frequency of the Hawking radiation mode assigned by the external observer it is reasonable to attribute a wavelength of l_P, the Planck length. In considering a black hole (BH) in equilibrium, it's understood that there are essentially two relevant length scales: the Schwarzschild radius and the Planck length. This equilibrium state is particularly pertinent for the emission of standard Hawking radiation, this is because a large black hole emits radiation very slowly, and the energy emitted in each instance is a minuscule fraction of the black hole's total mass.

An external observer would deduce that a Hawking mode emitted by the black hole has a source frequency of $\omega_{(\mathrm{H})}^{\mathrm{source}} = c/l_P$. To determine the frequency as it would be observed externally, this source frequency is redshifted and this redshifting process leads to the expected outcome, where the external frequency of the Hawking mode, $\omega_{(\mathrm{H})}^{\mathrm{ext}}$, is equal to the Hawking temperature T_H:

$$\omega_{(\mathrm{H})}^{\mathrm{ext}} = \omega_{(\mathrm{H})}^{\mathrm{source}} \sqrt{-g_{tt}}\bigg|_H = T_H. \tag{2.8}$$

From the perspective of the polymer model's internal dynamics, the same value for the Hawking temperature, denoted as T_H, is achieved. According to this model, a small loop of string, when it breaks away from longer loops within a bound state of interacting and highly excited closed strings, possesses a certain probability of escaping. Calculations within this framework demonstrate that both the rate and energy of this emission align with the Hawking temperature T_H. This result indicates a coherence between the external and internal perspectives in terms of understanding conventional Hawking radiation.

2.1.2 Supersized radiation

We shift our focus to a nonrelativistic fluid mode and its frequency as perceived by an external observer. It is understood that the redshift at the location of the protruding fluid, which is outside but near $r = R_S$, is given by $\frac{v_I}{c}$. This prompts us to consider the mode frequency at this "source" location.

An external observer, unaware of the fluid's existence, might misconstrue these nonrelativistic fluid modes as relativistic spacetime quasinormal modes (QNMs), at the source, these QNMs would have a wavelength roughly equal to R_S, as a result, one would attribute a source frequency to them as follows:

$$\omega_{(I)}^{\text{source}} = \frac{c}{R_S}, \tag{2.9}$$

leading to the inference that the external frequency is:

$$\omega_{(I)}^{\text{ext}} = \omega_{(I)}^{\text{source}} \sqrt{-g_{tt}}\Big|_I = \frac{v_I}{R_S}, \tag{2.10}$$

which aligns with the expectations. The primary distinction between the internal and external perspectives is, therefore, one of interpretation.

From the viewpoint of an external observer, supersized Hawking radiation is considered relativistic with a frequency $\omega_I = \frac{v_I}{R_S}$, it can therefore be deduced that the wavelength of this radiation, observed at a considerable distance from the horizon, is $\lambda_I = \frac{R_S c}{v_I}$. This conclusion is reinforced by the notion that the wavelength near the source should approximate R_S, and then experiences asymptotic redshifting to $\lambda_I \approx \frac{R_S c}{v_I}$.

Based on this, an external observer would infer a radial size of about R_S for the source. To comprehend the transmission cross-section for such long-wavelength modes through a relatively smaller surface area A, the observer would consider the ratio $\frac{A}{\lambda_I^2}$. For the scenario in question, this translates to $\frac{R_S^2}{\lambda_I^2} = v_I^2$.

Hence, we can conclude that the efficiency or coupling of emission is proportional to v_I^2, implying that the energy in the emitted wave is scaled as:

$$(\Delta E)_I \approx E_I v_I^2, \tag{2.11}$$

This assumption rests on the premise that the majority of the mode's energy is emitted as coherent waves, as opposed to being dissipated as heat.

The damping time for any particular mode, τ_I, is intrinsically linked to the corresponding relaxation time of the black hole. By examining the rate of change of energy, dE_I/dt, which is proportional to $(\Delta E)_I \approx v_I^2 E_I$, we find:

$$dE_I/dt \propto (\Delta E)_I \approx v_I^2 E_I, \tag{2.12}$$

indicating that the relaxation time scales inversely with v_I^2, as does the damping time τ_I. This leads to the anticipated result:

$$\tau_I \approx R_S/v_I^2, \tag{2.13}$$

where the inclusion of R_S is for dimensional consistency and acknowledges that the Schwarzschild time is the only classically relevant time scale.

In conclusion, supersized Hawking radiation oscillates at a frequency $\omega_I = v_I/R_S$, carries away energy $(\Delta E)I = E_I v_I^2$ (assuming $E_I \approx MBH$), and decays over a characteristic time $\tau_I = R_S/v_I^2$, this contrasts with standard Hawking emissions, which have a frequency $\omega_H = 1/R_S$, an effective coupling $v_H^2 = 1$ (comparable to $\omega_I = v_I/R_S$), and an emitted energy of $1/R_S$, resulting in a decay time $\tau_H = R_S/v_H^2 = R_S$, as expected. We now shift the attention to the strength of the coupling of fluid modes to external gravitational waves (GWs), which is also a key factor, as it, along with $(\Delta E)I$, determines the amplitude of the emitted GWs. The coupling strength can be estimated using Einstein's quadrupole formula:

$$hij \sim \frac{1}{r}\ddot{Q}, \tag{2.14}$$

which implies that for an external observer, the amplitude of the GWs, h_{ij}^I, is approximated as:

$$h_{ij}^I \sim \ddot{Q}_I \sim (\Delta E)_I R_S^2 \omega_I^2 \sim (E_I v_I^2)(R_S \omega_I)^2 \sim E_I v_I^4, \tag{2.15}$$

where the factor R_S^2 is attributed to the quadrupole moment of the emitting object, and the dot notation represents a time derivative. The inclusion of two frequency factors is due to the double time derivatives in the formula, which further suppresses the amplitude of the emitted GWs.

From the viewpoint of the internal dynamics of a black hole, the lack of relativistic fluid modes can be attributed to the polymer model being close to its equilibrium state due to a conflict between two necessary boundary conditions for any fluid mode: the requirement to vanish at the object's center and to be outgoing at its surface, additionally, the primary correction to the energy, $\Delta E/E$, must be parametrically small, as indicated by $\Delta E/E < 1$, this leads to the conclusion that $v_I^2/c^2 = \Delta E/E < 1$.

From an external viewpoint, the infeasibility of emitting such waves is evident when examining the continuity of emission at $v_I = 1$. Given that a sound velocity greater than 1 ($v_I > 1$) is physically untenable, the amplitude of any hypothetical waves surpassing light speed must be zero. By the principle of continuity, this leads to the conclusion that the amplitude of waves at $v_I = 1$ must also be zero.

To further clarify the continuity argument: a relativistic external mode could not have experienced redshift, as this would imply its origin from a fluid mode with a sound velocity surpassing the speed of light. For a hypothetical relativistic fluid mode, assume $\omega = \frac{\alpha c}{R_S}$ and $\lambda = \frac{R_S}{\alpha}$, where α is a constant, approximately of order 1, to account for any unconsidered numerical factors. If its wavelength is indeed $\frac{R_S}{\alpha} \approx R_S$, then the mode must

have originated near the horizon and thus undergone significant redshift. In contrast, to avoid redshift, it would need to be generated far from the horizon with a wavelength substantially greater than R_S. Such a mode would be independent of the black hole's influence and, even if it were to exist, an external observer would not categorize it as part of the black hole's quasinormal mode (QNM) spectrum. This logic, however, does not dispute the existence of standard relativistic spacetime QNMs, as these are a consequence of waves in the external spacetime, not from internal fluid modes of the black hole.

It has been demonstrated that for an ultracompact object with a surface effectively functioning as a black hole (BH) horizon, even if it's not empty, its interior modes can still interact with emitted gravitational waves (GWs), as well as other wave types like electromagnetic waves and neutrinos. An external observer would interpret these interior modes as enlarged Hawking emissions, seemingly originating just outside the horizon's equilibrium position. This perspective is applicable to both supersized and standard Hawking radiation.

These insights, primarily derived from studying the polymer model of a black hole's interior are believed to be generalizable. They likely extend to any ultracompact object that contains fluidlike matter and possesses an outer surface mimicking a BH horizon to a certain degree.

This concept leads to the notion of a new type of black hole hair, which necessitates a significantly extended period for shedding. The presence of such novel black hole hair could be a fundamental characteristic of any black hole-like object containing substantial matter. This could be the crucial element in unveiling the mysteries of what lies beyond the horizon. The detection of gravitational waves from black hole mergers, which might occur in the foreseeable future, could provide critical insights into this phenomenon.

2.1.3 No-hair theorems

The No-hair theorem posits that, absent external gravitational interactions, the geometry of a static black hole space-time is described by the Schwarzschild metric. However, this scenario is often not reflective of reality, as the prerequisites are seldom met. Typically, a black hole is part of a binary system or possesses an accretion disk, ensuring the presence of gravitational fields.

Nonetheless, the modified version of the no-hair theorem still holds true: The effect of the deformed black hole on the multipole moments, which describe the gravitational field near infinity and thus encompass all sources, is equivalent to that of a Schwarzschild black hole, this results in the Love number being zero, indicating no distortion for an extended object, and the absence of an induced multipole moment in the black hole. While these conclusions were initially drawn within an approximate framework of General Relativity, in [8] their validity is demonstrated in full General Relativity.

The No-hair theorem asserts that a static black hole is characterized by the Schwarzschild metric. Such a black hole, though it requires one parameter, or "hair", to be defined —

its mass M — is still considered "bald". For rotating black holes, an additional parameter, the spin, is necessary, but the essence of the theorem remains largely unchanged: a limited number of characteristics suffice to describe the space-time geometry of a black hole.

When applied to rotating black holes, the no-hair theorem stipulates that the quadrupole moment of such a black hole is inherently determined by its mass and angular momentum, therefore, the independent measurement of these three parameters can serve as a means to evaluate alternative theories of gravity or to scrutinize the fundamental principles of the no-hair theorem.

The no-hair theorem fundamentally posits that a black hole is an isolated entity, suggesting that its surrounding spacetime is inherently flat and devoid of external influences. Yet, this idealized condition often does not hold true in various astronomical situations, where factors like accretion disks or binary partners contribute to the spacetime's overall multipole moment.

In situations involving external sources within the black hole's vicinity, it experiences distortions, leading to changes in the internal structure of its horizon. These changes can be precisely evaluated using Love numbers of the first kind or by analyzing the multipole moments of isolated horizons. Importantly, however, these distortions don't necessarily mean black holes lose their characteristic 'hairlessness'. While the total multipole moments of spacetime observable from infinity are subject to change, these modifications arise solely from external sources, not from any inherent changes in the black holes themselves. Thus, even when distorted, black holes maintain only a mass monopole, effectively preserving their "baldness".

In an adiabatic regime, the black hole or neutron star is instantly distorted by the external field of its companion, the system then gains additional axial symmetry along the axis that connects the two components of the binary system. Under these circumstances, the metric for distorted black holes is applicable. The characteristics of these distortions are reflected in the gravitational waves emitted by spiraling binary systems, providing insights into the equation of state of neutron stars.

These imprints can serve as experimental evidence to determine whether a member of a binary system is a black hole, this method offers a direct way to confirm the presence of black holes. If the existence of a black hole in a binary system is already confirmed through other observations, like gamma-ray bursts observed at later stages of the inspiral, then analyzing its distortions through gravitational wave measurements provides an opportunity to test general relativity. This is done by applying the principles of the no-hair theorem. The distortions of the black holes and neutron stars are characterized by the Love numbers of first and second kind, h_r and k_r. Roughly speaking, the h_r measure the changes in the shape of the horizon or the neutron star and the k_r measure the change in the asymptotic multipole moments caused by the distortion due to an external source. It was established using approximation methods that the k_r vanish for four-dimensional black holes, but the black hole case considered by Gurlebeck is solved analytically in full

general relativity and, thus, it serves as a test for the various approximation schemes usually employed. In the following it is used the geometric units, in which $G = c = 1$, where c is the velocity of light and G Newton's gravitational constant. The metric has the signature $(-1, 1, 1, 1)$. Greek indices run from 0 to 3 and Latin indices run from 1 to 3.

2.1.4 Distorted BH

The representation of the metric for static and axially symmetric spacetimes of a general nature is achievable by using the Weyl metric, which is expressed as:

$$ds^2 = e^{2k-2U}(d\rho^2 + d\zeta^2) + W^2 e^{-2U} d\varphi^2 - e^{2U} dt^2 \tag{2.16}$$

Within this framework, the functions U, k, and W, which depend on ρ and ζ, are of high importance. The metric functions U and W can be defined in relation to the spacelike Killing vector η_α and the timelike Killing vector ξ_α, as follows:

$$e^{2U} = -\xi_\alpha \xi^\alpha, \quad W^2 = -\eta_\alpha \eta^\alpha \xi_\beta \xi^\beta. \tag{2.17}$$

When the external influences are either static and axially symmetric or suitable for a quasi-static analysis, the general metric in the proximity of a distorted black hole's horizon H was identified by Geroch and Hartle in the form resembling Eq. (2.16). Near H, the assumption of a pure vacuum is made, which is a physically justifiable supposition if the matter is quasi-static and adheres to the energy conditions. Accordingly, a surface S_H is defined, which encompasses H but excludes any additional sources. In cases where S_H is in close proximity to H, the metric functions, as delineated in Eq. (2.16), are expressed in the region between S_H and H as:

$$U = U_S + U_D, \quad k = k_S + k_{SD}, \quad W = \rho. \tag{2.18}$$

The function U_D is influenced by external matter and satisfies the Laplace equation:

$$\left(\frac{\partial^2}{\partial \rho^2} + \frac{1}{\rho} \frac{\partial}{\partial \rho} + \frac{\partial^2}{\partial \zeta^2} \right) U_D = 0. \tag{2.19}$$

In situations where U_D is zero, the spacetime is indicative of a Schwarzschild black hole. The computation of the function k_{SD} is conducted through a line integral, dependent on the combined values of $U_D + U_S$. However, its explicit expression is not crucial for subsequent discussions. The horizon of the distorted black hole is located along the symmetry axis ($\rho = 0, \zeta \in [-M, M]$), similar to a Schwarzschild black hole. In standard Weyl coordinates, the horizon is always at $\rho = 0$. These coordinates permit an adjustment of the ζ axis. By exploiting this flexibility, the horizon is symmetrically aligned with the ζ coordinate, meaning the 'north or south pole' of the horizon is represented by

$\zeta_{N/S} = \pm M$. At these extremities, U_D is required to have equivalent values to avoid the creation of struts, a simplification adopted for ease of analysis. For external matter that exhibits reflection symmetry, such as accretion disks or jets, this requirement is typically fulfilled.

The metric functions take on the form of Eq. (2.16) to (2.19) primarily in the proximity of H. These equations are not representative of the asymptotic behavior or the metric inside the external source, however, by employing source integrals, it is feasible to infer the contributions of the distorted black hole to the asymptotic multipole moments. This inference is possible even without a detailed description of the external sources, which may include additional black holes, the only condition imposed is that the spacetime should be asymptotically flat and all external sources must be confined within a certain region. This specified region should neither include H nor extend infinitely. The boundary of this region is designated as S_{ext}.

2.1.5 Source integrals

For distinguishing between the impacts of the black hole and external sources on the asymptotic multipole moments, the application of source integrals is essential, these integrals, recently formulated, facilitate the characterization of spacetime asymptotics, encompassing the Geroch multipole moments, by means of quasilocal surface or volume integrals. Such integrals are required to encircle or contain regions possessing a non-zero stress-energy tensor. In this scenario, the emphasis is on the surface integrals, with subsequent introduction of the relevant quantities.

Concerning the Weyl multipole moments $U^{(r)}$, the author defines them as the expansion of U along the axis of symmetry extending towards infinity, explicitly:

$$U = \sum_{r=0}^{\infty} \frac{U^{(r)}}{|\zeta|^{r+1}} \tag{2.20}$$

The coordinate ζ is both geometrically and covariantly definable. It is recognized that the Geroch multipole moments m_r can be determined from the values of $U^{(r)}$ through nonlinear algebraic relations. To derive m_r, it is essential to have knowledge of $U^{(k)}$ for all $0 \leq k \leq r$. Thus, the primary focus is directed towards $U^{(r)}$. It is important to note that the baseline for measuring the multipole moments is set by positioning $\zeta_{N/S} = \pm M$.

Additionally, the following functions are used

$$\begin{aligned} N_{-}^{(r)}(x,y) &= \sum_{k=0}^{\lfloor \frac{r}{2} \rfloor} \frac{2(-1)^{k+1} r! x^{2k+1} y^{r-2k}}{4^k (k!)^2 (r-2k)!} \\ N_{+}^{(r)}(x,y) &= \sum_{k=0}^{\lfloor \frac{r-1}{2} \rfloor} \frac{2(-1)^{k+1} r! x^{2k+2} y^{r-2k-1}}{4^k (k!)^2 (r-2k-1)!(2k+2)} \end{aligned} \tag{2.21}$$

It is straightforward to ascertain that these functions conform to the equations:

$$N^{(r)}_{+,x} - N^{(r)}_{-,y} = 0, \quad N^{(r)}_{+,y} + N^{(r)}_{-,x} - \frac{N^{(r)}_{-}}{x} = 0. \tag{2.22}$$

In this context, commas signify partial derivatives. The 1-form are here presented:

$$Z_\alpha = \epsilon_{\alpha\beta\gamma\delta} W^{,\beta} W^{-1} \eta^\gamma \xi^\delta, \tag{2.23}$$

with $\epsilon_{\alpha\beta\gamma\delta}$ representing the spacetime volume form.

In a vacuum setting, the characteristics of Z_α are clear, and it retains orthogonality to hypersurfaces across spacetime. Considering that the pertinent surfaces,

S_H and $S_{\rm ext}$, are situated either within the vacuum or at its boundary, the author introduces a scalar Z satisfying $Z_{,\alpha} = Z_\alpha$. It is observed that in the standard Weyl coordinates, Z is equivalent to ζ, assuming the integration constant is chosen correctly.

Under this established framework, the Weyl multipole moments are defined as:

$$\begin{aligned} U^{(r)} &= \int_{\mathcal{S}_\mathcal{H}} \eta^{(r)}_a \hat{n}^a \, \mathrm{d}\mathcal{S}_\mathcal{H} + \int_{\mathcal{S}_{\rm ext}} \eta^{(r)}_a \hat{n}^a \, \mathrm{d}\mathcal{S}_{\rm ext}, \\ \eta^{(r)}_a &= \frac{1}{8\pi} \frac{\mathrm{e}^U}{W} \left(N^{(r)}_{-} U_{,a} - N^{(r)}_{+,W} Z_{,a} U + N^{(r)}_{+,Z} W_{,a} U \right), \end{aligned} \tag{2.24}$$

Here, $\hat{n}_a$ symbolizes the unit normal vector directed outward from the surfaces S_H and $S_{\rm ext}$. The functions $N^{(r)}_{\pm}$ are associated with (x, y), corresponding to (W, Z). The expressions dS_H and $dS_{\rm ext}$ denote the proper area elements for S_H and $S_{\rm ext}$, respectively. In vacuum conditions, canonical Weyl coordinates are chosen, which allow for $W = \rho$ and $Z = \zeta$.

2.1.6 The induced multiple moment of disturbed BH

Using Eq. (2.24), the contributions from various sources to the asymptotic Weyl multipole moments can be distinguished in a covariant manner. The first component of Eq. (2.24), $U^{(r)}_H$, represents the influence from the distorted black hole. Conversely, the second component, $U^{(r)}_{\rm ext}$, relates to contributions from external sources, therefore, the resulting multipole moment caused by a distorted black hole is defined as $U^{(r)}_{\rm ind} = U^{(r)}_H - U^{(r)}_S$, where $U^{(r)}_S$ denotes the Weyl multipole moments of an undistorted Schwarzschild black hole, which align with the Newtonian multipole moments for a uniform density line mass. For S_H parameterized at constant angles ϕ, extending from the "north pole" to the "south pole" ($s \in [s_N, s_S] \to (\rho(s), \zeta(s), \phi = \text{const.})$), the author calculates $U^{(r)}_H$ by employing Eq. (2.18):

$$U_{\mathcal{H}}^{(r)} = \frac{1}{4}\int_{s_N}^{s_S} \Big[N_{-}^{(r)}\left(U_S + U_D\right)_{,n} - \left(N_{+,W}^{(r)} Z_{,n} - N_{+,Z}^{(r)} W_{,n}\right)\left(U_S + U_D\right)\Big]\,\mathrm{d}s, \tag{2.25}$$

In this expression, $f_{,n}$ denotes the normal derivative, defined as $-f_{,\rho}\frac{d}{ds}\zeta(s)+f_{,\zeta}\frac{d}{ds}\rho(s)$. To determine the multipole moments of a Schwarzschild black hole, one can reference Eq. (2.25) and set $U_D = 0$. For calculating the induced multipole moments, the Schwarzschild contribution is simply subtracted from Eq. (2.25), yielding:

$$U_{\mathrm{ind}}^{(r)} = \frac{1}{4}\int_{s_N} \Big[N_{-}^{(r)} U_{D,n} - N_{+,W}^{(r)} Z_{,n} U_D + N_{+,Z}^{(r)} W_{,n} U_D\Big]\,\mathrm{d}s. \tag{2.26}$$

Employing the divergence theorem and Eq. (2.19), $U_{\mathrm{ind}}^{(r)}$ can be rewritten:

$$U_{\mathrm{ind}}^{(r)} = \frac{1}{8\pi}\int_{V_{\mathcal{H}}} \frac{1}{\rho}\left[U_{D,\rho}\left(N_{-,\rho}^{(r)} + N_{+,\zeta}^{(r)} - \frac{N_{-}^{(r)}}{\rho}\right) + U_{D,\zeta}\left(N_{-,\zeta}^{(r)} - N_{+,\rho}^{(r)}\right)\right]\mathrm{d}V_{\mathcal{H}}, \tag{2.27}$$

This formulation is nullified according to the stipulations of Eq. (2.22). Here, V_H symbolizes the coordinate volume enclosed by S_H and H within the canonical Weyl coordinates. As a result, the induced multipole moments are effectively nullified, leading to the deduction that the contributions of the distorted black hole to the asymptotic Weyl multipole moments are analogous to those of a Schwarzschild black hole. By incorporating insights from additional research, these conclusions can be extended to Geroch's multipole moments, thus expanding the no-hair theorem's applicability to include black holes affected by external matter. It is pertinent to acknowledge that this external matter also contributes to the gravitational field, meaning that the aggregate asymptotic multipole moments often differ from those of a pure Schwarzschild spacetime. This deviation is particularly pronounced in binary black hole systems. In the discussed analysis, the reference for the measurement of multipole moments is centered on one black hole, treating the other as external matter. This approach results in additional contributions, such as a non-zero quadrupole moment, to the overall multipole moments, as indicated after Eq. (2.20).

The nonexistence of induced multipole moments implies that the second Love numbers k_r are likewise zero, being directly proportional to $U_{\mathrm{ind}}^{(r)}$. This finding aligns with previously established research, highlighting that it is derived without any simplifications or linearizations, thus maintaining validity within the framework of full general relativity. It seems appropriate to assume $k_r = 0$ for slowly rotating black holes within

binary systems, particularly when calculating gravitational radiation during the adiabatic phase. It is important to note that the characteristic of $k_r = 0$ is distinct to black holes and does not extend to neutron stars. Nonetheless, the source integrals for the Weyl multipole moments are meticulously constructed to calculate their k_r, facilitating the separation of contributions from various sources to the Weyl multipole moments in a covariant approach under general relativity. This aspect significantly eases the computation of the source integrals in contexts involving black holes, as it suffices to determine the mass of each black hole to establish all $U_H^{(r)}$.

If black holes rotate sufficiently slowly, this bears significant consequences in astrophysics. On one hand, the determination of a black hole's mass directly defines its contribution to the multipole moments. In scenarios like binary systems involving a black hole, or a black hole with an accretion disk, the black hole's mass can be estimated from the total mass of the system, which is derived from the motion of remote stars and the mass of either the companion star or the disk. Once the black hole's mass is ascertained, all its associated multipole moments are effectively set. Any measurement of the entire system's multipole moments, for instance, the quadrupole moment, essentially determines the quadrupole moment of the companion or the disk. On the other hand, if it's possible to measure the quadrupole moments of both the entire system and the companion star or disk, then such observations offer a means to validate the principles of general relativity.

2.1.7 The multiple moments of the horizon

Although the distorted black hole exhibits the same asymptotic multipole moments as a Schwarzschild black hole, significant alterations are observed in its horizon geometry, this becomes apparent when analyzing the covariantly defined horizon multipoles M_n. The same principle was also independently applied using coordinate systems akin to those of Schwarzschild, it was found that the multipole moments of the distorted horizon differ from those of a standard Schwarzschild black hole. These differences were crucial in developing a relativistic analogue to the first Love numbers for black holes, which, unlike the second Love numbers, are non-zero.

Despite these changes in horizon geometry, the asymptotic multipole moments do not reflect them, this paradoxical situation can be understood through a simple Newtonian analogy. Consider a point mass: all its multipole moments, except for its mass, are null, and its equipotential surfaces are spherical, introducing an additional gravitational field from another point mass changes the equipotential surfaces, but the multipole moments of the original mass, as calculated by Newtonian source integrals, remain the same. This is attributed to the fact that a point particle, lacking internal structure, cannot be distorted by external gravitational forces; hence, its source remains consistent. The equipotential surfaces, similar to the distorted horizon, become non-spherical, however, this changes if the body has internal structure, as with neutron stars. In such cases,

an external gravitational field can deform both the matter distribution and the sources, effects that are observable in the asymptotic multipole moments.

2.2 Parallelism with the electric polarizability problem

This section based on the perturbation theory chapter in Griffiths [4] introduces the necessary elements of perturbation theory to understand the computations of the main article.

2.2.1 Perturbation theory

Initially, we present the modified Hamiltonian as a composite of two distinct elements:

$$H = H^0 + \lambda H', \tag{2.28}$$

where H' is identified as the perturbative component. We consider λ a small value, expanding ψ_n and E as a series in terms of λ, we get

$$\psi_n = \psi_n^0 + \lambda\psi_n^1 + \lambda^2\psi_n^2 + \cdots ; \quad E_n = E_n^0 + \lambda E_n^1 + \lambda^2 E_n^2 + \cdots , \tag{2.29}$$

Here, E_n^1 is the first order correction to the n^{th} eigenvalue, and ψ_n^1 is the first order correction to the n^{th} eigenfunction; the terms E_n^2 and ψ_n^2 represent the second-order corrections, and the progression continues. Plugging equations (2.28), (2.29), and (2.30) into

$$H\psi_n = E_n\psi_n, \tag{2.30}$$

, we get

$$\begin{aligned} &\left(H^0 + \lambda H'\right)\left[\psi_n^0 + \lambda\psi_n^1 + \lambda^2\psi_n^2 + \cdots\right] \\ &= \left(E_n^0 + \lambda E_n^1 + \lambda^2 E_n^2 + \cdots\right)\left[\psi_n^0 + \lambda\psi_n^1 + \lambda^2\psi_n^2 + \cdots\right], \end{aligned} \tag{2.31}$$

and by collecting terms with similar powers of λ, we obtain

$$\begin{aligned} &H^0\psi_n^0 + \lambda\left(H^0\psi_n^1 + H'\psi_n^0\right) + \lambda^2\left(H^0\psi_n^2 + H'\psi_n^1\right) + \cdots \\ &= E_n^0\psi_n^0 + \lambda\left(E_n^0\psi_n^1 + E_n^1\psi_n^0\right) + \lambda^2\left(E_n^0\psi_n^2 + E_n^1\psi_n^1 + E_n^2\psi_n^0\right) + \cdots . \end{aligned} \tag{2.32}$$

At first order (λ^0), we encounter $H^0\psi_n^0 = E_n^0\psi_n^0$, which is a familiar result and merely reaffirms our initial equation. Moving to the first order (λ^1),

$$H^0\psi_n^1 + H'\psi_n^0 = E_n^0\psi_n^1 + E_n^1\psi_n^0. \tag{2.33}$$

Proceeding to the second order (λ^2),

$$H^0\psi_n^2 + H'\psi_n^1 = E_n^0\psi_n^2 + E_n^1\psi_n^1 + E_n^2\psi_n^0, \tag{2.34}$$

and this pattern continues.

2.2.2 First-Order Theory

Computing the inner product of our equation with ψ_n^0 (in other words, multiplying by $(\psi_n^0)^*$ and integrating),

$$\left\langle \psi_n^0 \mid H^0\psi_n^1 \right\rangle + \left\langle \psi_n^0 \mid H'\psi_n^0 \right\rangle = E_n^0 \left\langle \psi_n^0 \mid \psi_n^1 \right\rangle + E_n^1 \left\langle \psi_n^0 \mid \psi_n^0 \right\rangle \tag{2.35}$$

Given that H^0 is Hermitian, it follows that

$$\left\langle \psi_n^0 \mid H^0\psi_n^1 \right\rangle = \left\langle H^0\psi_n^0 \mid \psi_n^1 \right\rangle = \left\langle E_n^0\psi_n^0 \mid \psi_n^1 \right\rangle = E_n^0 \left\langle \psi_n^0 \mid \psi_n^1 \right\rangle, \tag{2.36}$$

which eliminates the first term on the right side. Additionally, $\langle \psi_n^0 \mid \psi_n^0 \rangle = 1$, leading to

$$E_n^1 = \left\langle \psi_n^0 \left| H' \right| \psi_n^0 \right\rangle \tag{2.37}$$

This presents the cornerstone of first-order perturbation theory; in practical terms, it might be regarded as one of the most crucial equations in quantum mechanics. Essentially, it conveys that the primary correction to energy is the expected value of the perturbation in the original, undisturbed state.

The key to finding the first-order correction to the wave function lies in reinterpreting our equation (2.33):

$$\left(H^0 - E_n^0\right)\psi_n^1 = -\left(H' - E_n^1\right)\psi_n^0. \tag{2.38}$$

Here, the right side represents a known quantity, leading us to an inhomogeneous differential equation for ψ_n^1. Given that the unperturbed wave functions form a complete set, we can express ψ_n^1 (or any other function) as their linear combination:

$$\psi_n^1 = \sum_{m\neq n} c_m^{(n)}\psi_m^0 \tag{2.39}$$

(We exclude $m = n$ in this summation because if ψ_n^1 satisfies our equation, so does $(\psi_n^1 + \alpha\psi_n^0)$ for any constant α, allowing us to omit the ψ_n^0 term). Determining the coefficients $c_m^{(n)}$ is our objective, by incorporating this equation into our previous one and utilizing the fact that ψ_m^0 satisfies the original Schrödinger equation, the following relation can be established:

$$\sum_{m\neq n}\left(E_m^0 - E_n^0\right)c_m^{(n)}\psi_m^0 = -\left(H' - E_n^1\right)\psi_n^0. \tag{2.40}$$

Upon computing the inner product with ψ_l^0,

$$\sum_{m\neq n}\left(E_m^0 - E_n^0\right)c_m^{(n)}\left\langle \psi_l^0 \mid \psi_m^0 \right\rangle = -\left\langle \psi_l^0 \left| H' \right| \psi_n^0 \right\rangle + E_n^1\left\langle \psi_l^0 \mid \psi_n^0 \right\rangle. \tag{2.41}$$

In cases where $l = n$, the left side amounts to zero, leading us back to our fundamental equation; for $l \neq n$, the result is

$$\left(E_l^0 - E_n^0\right) c_l^{(n)} = -\left\langle \psi_l^0 \left| H' \right| \psi_n^0 \right\rangle, \tag{2.42}$$

which can be rearranged as

$$c_m^{(n)} = \frac{\left\langle \psi_m^0 \left| H' \right| \psi_n^0 \right\rangle}{E_n^0 - E_m^0} \tag{2.43}$$

thus leading to the expression

$$\psi_n^1 = \sum_{m \neq n} \frac{\left\langle \psi_m^0 \left| H' \right| \psi_n^0 \right\rangle}{(E_n^0 - E_m^0)} \psi_m^0 \tag{2.44}$$

2.2.3 Second-Order Energies

Following the previous method, we compute the inner product of the second-order equation with ψ_n^0 :

$$\left\langle \psi_n^0 \mid H^0 \psi_n^2 \right\rangle + \left\langle \psi_n^0 \mid H' \psi_n^1 \right\rangle = E_n^0 \left\langle \psi_n^0 \mid \psi_n^2 \right\rangle + E_n^1 \left\langle \psi_n^0 \mid \psi_n^1 \right\rangle + E_n^2 \left\langle \psi_n^0 \mid \psi_n^0 \right\rangle \tag{2.45}$$

Utilizing the Hermiticity of H^0 again:

$$\left\langle \psi_n^0 \mid H^0 \psi_n^2 \right\rangle = \left\langle H^0 \psi_n^0 \mid \psi_n^2 \right\rangle = E_n^0 \left\langle \psi_n^0 \mid \psi_n^2 \right\rangle, \tag{2.46}$$

this negates the first term on the left with the first term on the right. Since $\langle \psi_n^0 \mid \psi_n^0 \rangle = 1$, we arrive at an equation for E_n^2 :

$$E_n^2 = \left\langle \psi_n^0 \left| H' \right| \psi_n^1 \right\rangle - E_n^1 \left\langle \psi_n^0 \mid \psi_n^1 \right\rangle \tag{2.47}$$

However,

$$\left\langle \psi_n^0 \mid \psi_n^1 \right\rangle = \sum_{m \neq n} c_m^{(n)} \left\langle \psi_n^0 \mid \psi_m^0 \right\rangle = 0 \tag{2.48}$$

leads us to

$$E_n^2 = \left\langle \psi_n^0 \left| H' \right| \psi_n^1 \right\rangle = \sum_{m \neq n} c_m^{(n)} \left\langle \psi_n^0 \left| H' \right| \psi_m^0 \right\rangle = \sum_{m \neq n} \frac{\left\langle \psi_m^0 \left| H' \right| \psi_n^0 \right\rangle \left\langle \psi_n^0 \left| H' \right| \psi_m^0 \right\rangle}{E_n^0 - E_m^0}, \tag{2.49}$$

and finally,

$$E_n^2 = \sum_{m \neq n} \frac{\left| \left\langle \psi_m^0 \left| H' \right| \psi_n^0 \right\rangle \right|^2}{E_n^0 - E_m^0} \tag{2.50}$$

This formula is effectively the same used for computing the polarizability of an atom and the second Love number as presented in the next section, the only difference is that in the next section the wavefunctions have the presence of the angular part manifested with spherical harmonics.

2.3 Classical Love number

In this section we follow the work of Ram Brustein and Yotam Sherf in [4] illustrating the framework and the computation of the second Love number using a model based on non-relativistic fluids.

The process of binary system inspiral involves mutual tidal interactions, causing distortions in the spherical mass distribution of the system. These tidal responses are measured using tidal Love numbers, which distinctly affect the gravitational wave (GW) signals emitted. In the framework of general relativity (GR), it is established that black holes (BHs) exhibit zero Love numbers, an outcome of the BH no-hair theorem exposed in the last chapter.

The upcoming Laser Interferometer Space Antenna (LISA) observations of GWs from binary BH mergers during their inspiral phase could serve as a means to investigate the quantum characteristics of large-scale astrophysical BHs through the influence of these characteristics on the GW signals. This premise hinges on the assertion that the "electric" quadrupolar Love number, k2, is nonzero for a quantum black hole (QBH). This nonzero value of k2, especially since it is the most significant among the dimensionless Love numbers and contrasts with its zero value in classical GR BHs, presents a crucial indicator for potential deviations from classical GR.

The primary focus is on determining the Love numbers for large astrophysical black holes (BHs). In line with the Bohr correspondence principle, which is applicable to all macroscopic objects, there should exist a quantum state corresponding to a classical BH, irrespective of its size. This idea is captured by the term "quantum black hole" (QBH), which refers to the quantum state analogous to a classical BH. A QBH is described as an ultracompact object with a horizon and a unique set of quantum mechanical energy levels, these levels can be seen as coherent states representing the macroscopic, semiclassical excitations of the QBH. For example, in the polymer BH model, the interior matter of a QBH is thought to behave like a fluid, capable of supporting pulsating modes similar to those in a relativistic star.

Beyond the standard spacetime modes in the exterior, these fluid modes would also be present, thereby requiring their inclusion in the spectrum of ringdown or quasinormal modes of a perturbed BH. Each fluid mode, when stimulated, forms a high-amplitude, high occupation number, coherent state of the interior matter, rather than a single quantum excitation. In the ground state of a QBH, the external geometry closely matches that of Schwarzschild geometry. However, an excited QBH shows deviations from its General Relativity (GR) description, potentially allowing for its differentiation from a classical counterpart in theory. This distinction is valid as long as the QBH is somewhat out of its equilibrium state, in contrast to a GR BH, with the degree of deviation being contingent on the energy input into each specific mode.

To differentiate between a QBH and a classical BH, one can observe them when they are slightly out of equilibrium due to the external field of a binary companion.

The classical BH lacks any features (bald), whereas the quantum BH exhibits quantum characteristics (hair). Commonly, it's believed that quantum effects in large astrophysical BHs are minimal due to the very small ratio of the Planck length squared to typical curvatures l_P^2/R_S^2. However, it's argued that for QBHs, quantum effects are determined by the extent of the quantum hair, which could be significantly larger. For instance, in string theory, the dimensionless magnitude of this hair is proportional to the square of the string coupling, $g_s^2 \approx l_s^2/l_P^2$, with l_s being the string length. Generally, g_s^2 is small but comparable to other typical gauge couplings, roughly $g_s^2 \approx 0.1$.

In classical general relativity (GR), a black hole (BH) geometry does undergo deformation when exposed to an external perturbing field, this deformation howeveer, is not due to a change in matter distribution but is represented by a variation in the Gaussian curvature at the Schwarzschild radius, or equivalently, in the scalar curvature. This deformation can be conceptualized by embedding the BH in a hypothetical two-dimensional sphere, leading to the interpretation of deformation as a relative radial shift at the Schwarzschild radius, nevertheless, this geometric deformation should not be mistaken for a tangible physical effect. For an observer near the BH, the horizon remains at the Schwarzschild radius, If this were not the case, it would imply a nonzero Love number. It has been elucidated that the geometrical deformations of classical BHs do not translate into changes in their asymptotic multipole moments, thus resulting in an identically zero Love number. The key takeaway is that a discernible imprint on the object's asymptotic moment necessitates a genuine physical matter deformation, or in other words, an actual response of the state of the quantum black hole (QBH) to external perturbations.

When addressing the significance of quantum hair for the calculation of k2, it is important to emphasize that from the perspective of an external observer, the interior of the ultracompact object influences the outcome solely through one boundary condition (BC) applied to the external Einstein equations at the object's surface. The second BC is defined exclusively by the perturbing classical field at a significant distance from the object, therefore the interior details of the object, including its composition, energy density, or pressure, are encapsulated in this single BC, as the interior essentially becomes integrated out of the equations (this connects to what was discussed in "The external point of view"). The Love number is calculated based on the ratio of these two BCs. Thus, any information about the interior that is available to an outside observer is conveyed through the Love number(s).

2.3.1 Quantum Love number review

Given the inaccessibility of the QBH's interior to an external observer and the assumption of strong internal gravitational coupling, the conventional approach of a semiclassical geometric description using curved spacetime becomes untenable. However, the central point concerning the QBH interior is the macroscopic nature of its excitations, which

justifies the application of the Bohr correspondence principle. This principle suggests that the excited spectrum of a QBH can be described using coherent states, corresponding to semiclassical states that function analogously to an oscillating classical system. These assumptions enable the discussion of the macroscopic excitations and energy spectrum of a quantized black hole using a harmonic oscillator model.

To conceptualize this idea, the exotic matter within the QBH is envisaged as a fluid capable of sustaining pulsating modes, akin to those found in a relativistic star. These fluid modes exist alongside the standard spacetime modes in the exterior. The perturbations are classified into fluid modes and spacetime modes. Due to the low sound speed of the fluid modes and the compactness of the QBH, these modes are distinguished from spacetime perturbations, as per the Cowling approximation.

To frame the calculation of the Love number for a quantum black hole (QBH), an analogy can be drawn with the process of determining the polarizability of an atom. Envision an atom in its fundamental state, represented by $|\Psi_0\rangle$, which is characterized by specific quantum numbers $|n;l;m\rangle = |1;0;0\rangle$. It is presumed that the expectation value of the quantum dipole operator $\hat{D}_i$ is null in this state. From a classical standpoint, the dipole moment is defined as $\vec{D} = \int \rho(\vec{x}_0)\vec{x}_0 dV_0 = 0$, where ρ denotes the atom's charge density. This conceptual framework aids in understanding the Love number's computation for QBH, using familiar quantum mechanical principles applied to atomic structures.

When the atom is situated in a region with a nearly uniform electric field E_i, resulting from a weak external potential $U_{\rm ext}$, the electric field can be expressed as $E_i = \frac{\partial U_{\rm ext}}{\partial x_i}$. The interaction between the atom and the external electric field, $\hat{V}_{\rm int}$, is described in terms of $\hat{D}_i$, specifically, $\hat{V}_{\rm int} = -E_i\hat{D}_i$. The induced dipole moment of the atom, perturbed by this interaction and calculated using second-order time-independent perturbation theory, is given by the standard formula, also shown before:

$$\left\langle \Psi_0 \left| \hat{D}_j \right| \Psi \right\rangle = -\mathcal{E}_i \sum_{n\neq 1,l,m} \frac{\left\langle 1,0,0 \left| \hat{D}_i \right| n,l,m \right\rangle \left\langle n,l,m \left| \hat{D}_j \right| 1,0,0 \right\rangle}{\Delta E_{1,n}}, \tag{2.51}$$

where $\Delta E_{1,n} = E_1 - E_n$. In this scenario, symmetry dictates that $l = 1$ and $m = -1, 0, 1$, with $i = j$. The atom's linear response to the external electric field is represented as $\langle\Psi_0|\hat{D}_i|\Psi_0\rangle = \alpha\mathcal{E}_i$, where α denotes the electric polarizability, given by

$$\alpha = \sum_{n\neq 1,m\pm 1,0,1} \frac{\left|\langle 1,0,0|\hat{D}_i|n,1,m\rangle\right|^2}{\Delta E_{1,n}}. \tag{2.52}$$

Drawing parallels to these principles, to obtain the Love numbers one needs to replace the electric field and dipole moment with tidal fields and mass moments. For the quantum

calculation, the inspiral phase of a binary system is considered, similar to the classical computation. In this system, one companion is a QBH of mass M_{BH} and radius $R_S = 2M_{BH}$, while the other is an external object of mass M_{ext} orbiting at radius b. During the early stages of inspiral, the QBH responds to the gradually changing tidal field produced by its companion. For $b \gg R_S$, the Newtonian potential of the external body, $U_{ext} = -M_{ext}/|\vec{b} - \vec{x}|$, can be expanded in the QBH's local inertial frame as $U_{ext}(t, \vec{x}) = U_{ext}(0) + \frac{1}{2}\frac{\partial^2 U_{ext}}{\partial x_i \partial x_j}\big|_0 x_i x_j + \ldots$.

Analogous to the case of electric polarizability, the interaction of the QBH with the external field is quantified in terms of the mass moment expectation value, $\hat{Q}(l)$. These operators are the quantum analogues of classical symmetric trace-free mass multipoles. It is assumed that in the BH ground state, denoted as $|\Psi_0\rangle$, the expectation value of the BH mass moment is zero, in accordance with the spherical symmetry and classical no-hair properties, i.e., $\langle\Psi_0|\hat{Q}(l)|\Psi_0\rangle = 0$. Given the slow and weak nature of the external potential, time-independent perturbation theory serves as an effective approximation.

In previous research, the correction to the ground state energy of a nonrotating quantum black hole (QBH) due to the induced quadrupole was evaluated, $\hat{Q}_{ij}$, where the Schwarzschild radius is R_S. Recall that in the classical framework, $Q_{ij} = \int \rho(t, x')(x'_i x'_j - \frac{1}{3} r^2 \delta_{ij}) dV'$, with ρ representing the energy density. Analogous to the electric polarizability calculation, the interaction energy is defined as $\hat{V}_{\text{int}} = -\frac{1}{2}\mathcal{E}_{ij}\hat{Q}_{ij}$, where $\mathcal{E}_{ij} = \frac{\partial^2 U_{\text{ext}}}{\partial x^i \partial x^j}$.

The leading-order corrections to the QBH ground state quadrupole in second-order time-independent perturbation theory are described by

$$\langle\Psi_0|\hat{Q}_{kl}|\Psi_0\rangle = \mathcal{E}_{ij} \sum_{n>1,l,m} \frac{\langle\Psi_0|\hat{Q}_{ij}|n,l,m\rangle\langle n,l,m|\hat{Q}_{kl}|\Psi_0\rangle}{|\Delta E_{1,n}|}, \tag{2.53}$$

where $|\Delta E_{1,n}| = E_n - E_1$. The ground state Ψ_0 has a radial number denoted by $n = 1$, thus the energy of the ground state is $E_1 = M_{\text{BH}}$. This is consistent with standard treatments of second-order perturbation theory. The "electric" quadrupolar Love number is the proportionality coefficient between the induced electric quadruple moment and the external tidal field,

$$\langle\Psi_0|\hat{Q}_{ij}|\Psi_0\rangle = -\lambda_2 \mathcal{E}_{ij}. \tag{2.54}$$

Here, λ_2 represents the dimensional quadrupolar Love number, and its dimensionless form is commonly defined as $k_2 = \frac{3}{2}R^{-5}\lambda_2$. It can be derived that

$$k_2 = -\frac{3}{4R^5} \sum_{n,-2<m<2} \frac{|\langle\Psi_0|\hat{Q}_{ij}|n,2,m\rangle|^2}{|\Delta E_{1,n}|}. \tag{2.55}$$

2.4 Explicit internal solution for the metric

The response of a celestial body to a weak external tidal field is manifest in its induced mass (electric) and current (magnetic) moments. The focus here is on the quadrupolar

"electric" Love number k_2. At a considerable distance, in the local asymptotic rest frame of the star, the temporal component of the metric is given by:

$$\begin{aligned} g_{tt} &= -1 + \frac{2M}{r} - \mathcal{E}_{ij}x^i x^j + 3\frac{1}{r^5}Q_{ij}x^i x^j \\ &= -1 + \frac{2M}{r} - \mathcal{E}_{ij}x^i x^j - 2k_2\left(\frac{R}{r}\right)^5 \mathcal{E}_{ij}x^i x^j, \end{aligned} \tag{2.56}$$

where M and R are the mass and radius of the star, respectively. The dimensionless tidal Love number k_2 measures the linear response to the applied field. In the deviation of g_{tt} from the Schwarzschild metric, the first term describes the applied tidal field, while the term proportional to k_2 represents the induced trace-free quadrupole moment $Q_{ij} = \int d^3x\, \rho(x)\left(x_i x_j - \frac{1}{3}\delta_{ij}r^2\right)$,

$$Q_{ij} = -\frac{2}{3}k_2 R^5 \mathcal{E}_{ij}. \tag{2.57}$$

In a Newtonian framework, at large distances, $g_{tt} = -(1 + 2U_N)$. Expanding the Newtonian potential U_N to the second order in the body's local inertial frame gives

$$U_N = -\frac{M}{r} - \frac{3}{2r^5}Q_{ij}x^i x^j + \frac{1}{2}\mathcal{E}_{ij}x^i x^j \tag{2.58}$$

with E_{ij} being the quadrupole moment of the external potential $\mathcal{E}_{ij} = \frac{\partial^2 U_{\text{ext}}}{\partial x_i \partial x_j}$. In the case of an axisymmetric external potential, the tidal field is represented by $\mathcal{E}_{ij}x^i x^j = \mathcal{E}r^2 Y_{20}$, and similarly, the induced moment follows the same angular dependence, $Q_{ij} = QY_{20}$. Therefore, it follows that

$$U_N = -\frac{M}{r} - \frac{3}{2r^3}QY_{20} + \frac{1}{2}\mathcal{E}r^2 Y_{20}, \tag{2.59}$$

and

$$\begin{aligned} g_{tt} &= -1 + \frac{2M}{r} + 3Q\frac{1}{r^3}Y_{20} - \mathcal{E}r^2 Y_{20}, \\ &= -1 + \frac{2M}{r} - 2k_2 R^5 \mathcal{E}\frac{1}{r^3}Y_{20} - \mathcal{E}r^2 Y_{20}, \end{aligned} \tag{2.60}$$

with

$$k_2 R^5 = -\frac{3}{2}\frac{Q}{\mathcal{E}}. \tag{2.61}$$

In [6] is then shown the calculation of the Love number k_2, considering a perturbation $h_{\mu\nu}$ about the Schwarzschild background $g^{(0)}_{\mu\nu}$, where $g^{(0)}_{\mu\nu} = \text{diag}(-e^{\nu(r)}, e^{\lambda(r)}, r^2, r^2\sin^2\theta)$, and $e^{\nu(r)} = e^{-\lambda(r)} = 1 - 2M/r$. The perturbation $h_{\mu\nu}$ is decomposed into even-parity and odd-parity parts, following the Regge-Wheeler gauge. Focusing on the $l = 2, m = 0$

term, to linear order, when the external field is static ($\mathcal{E}$ = const.), the even-parity perturbations can be expressed as

$$h_{\mu\nu} = \mathrm{diag}\left(e^{\nu(r)}H_0(r), e^{\lambda(r)}H_2(r), r^2K(r), r^2\sin^2\theta K(r)\right) Y_{20}. \tag{2.62}$$

Upon solving the perturbed Einstein equations outside the celestial body, it is found that $H_0 = H_2 \equiv H(r)$. This leads to the following perturbation equations:

$$H'' + \frac{2x}{x^2-1}H' - \frac{6x^2-2}{(x^2-1)^2}H = 0, \tag{2.63}$$

$$\begin{aligned} K' - H' - \frac{2}{(x^2-1)}H &= 0, \\ K - \frac{1}{2}H' - \frac{1}{4}\left(\frac{x+1}{x-1} + \frac{3x+5}{x+1}\right)H &= 0, \end{aligned} \tag{2.64}$$

where $x = \frac{r}{M} - 1$ and the prime denotes a derivative with respect to x.

The external solution of these perturbation equations is given by

$$\begin{aligned} H_{\mathrm{ext}}(x) = c_1 &\left[\frac{x(5-3x^2)}{x^2-1} + \frac{3}{2}(x^2-1)\ln\left(\frac{x+1}{x-1}\right)\right] \\ &+ 3c_2(x^2-1), \end{aligned} \tag{2.65}$$

$$\begin{aligned} K_{\mathrm{ext}}(x) = -c_1&\frac{4+3x(x+3)}{x+1} + \frac{3}{2}c_1(x^2+2x-1)\ln\left(\frac{x+1}{x-1}\right) \\ &+ 3c_2(x^2+2x-1), \end{aligned} \tag{2.66}$$

and the perturbed background metric by

$$g_{tt} = -\left(\frac{x-1}{x+1}\right)\left(1 + H_{\mathrm{ext}}Y_{20}\right). \tag{2.67}$$

The main focus is on cases where $x - 1 = \frac{r}{M} - 2$ is significantly less than 1. For subsequent analysis, H_{ext} and K_{ext} are expanded in this limit, resulting in:

$$H_{\mathrm{ext}}(x) = \frac{c_1}{x-1} - 3c_1\ln\left(\frac{x-1}{2}\right) + 6c_2(x-1) + \mathcal{O}(x-1), \tag{2.68}$$

thereby laying the groundwork for further investigation into the perturbative aspects of the gravitational field around celestial bodies. Additionally, the expansion of $K_{\mathrm{ext}}(x)$ in the same limit is given by:

$$K_{\mathrm{ext}}(x) = -8c_1 - 3c_1\ln\left(\frac{x-1}{2}\right) + 6c_2 + \mathcal{O}(x-1). \tag{2.69}$$

To facilitate the analysis, the coefficients of the expanded metric namely $\mathcal{E}$ and k_2, are related to the coefficients c_1 and c_2, as follows:

$$c_1 = 40M^2 k_2 \mathcal{E} \tag{2.70}$$

and

$$c_2 = \frac{1}{3} M^2 \mathcal{E}, \tag{2.71}$$

resulting in

$$k_2 = \frac{1}{120} \frac{c_1}{c_2}. \tag{2.72}$$

The form of the external solution, as outlined in Eq. (2.65), is independent of the interior characteristics, given that it represents a vacuum solution of the Einstein equations. The constant c_2 is determined solely by the external field, thus the only implicit dependence of H_{ext} on the interior lies in the ratio c_1/c_2, or equivalently, in the value of k_2. Therefore, to completely define the form of the external metric perturbations, an additional boundary condition on H_{ext} needs to be established.

The standard method for calculating k_2 for objects with known and defined interiors is detailed in the relevant literature. This approach starts with specifying the internal configuration of the perturbed body using its stress-energy-momentum tensor and an equation of state. The perturbed Einstein equations within the interior are then solved to find H_{int}. The conditions for H_{int} to be regular at the star's center ($r = 0$) and for the continuity of H and K at the star's surface ($r = R$) lead to the determination of the coefficients c_1 and c_2, and subsequently k_2.

This method, which requires a full solution of the interior to calculate k_2, provides more information than necessary if the goal is simply to determine k_2. Since only the ratio of two numbers is essential for k_2, any alternative method that can define this ratio would be as effective as the conventional approach.

2.5 Spectrum of non-relativistic fluids

In the realm of astrophysical interactions, the entity under scrutiny, referred to as the "primary," is subjected to a weak periodic force exerted by its companion. Fluid modes of ultracompact objects can be represented as a series of driven harmonic oscillators, each with distinct frequencies. Within this effective model, the interior modes are perceived by an asymptotic observer as nonrelativistic (NR) fluid modes, with an analysis akin to that of classical Newtonian NR fluid modes.

Owing to the low sound speed and the compact nature of the quantum black hole (QBH), fluid modes are effectively isolated from spacetime perturbations, this leads to a division of the internal perturbation into two separate categories: the fluid modes and the spacetime modes.

The oscillating modes of the object are characterized by radial and spherical indices n, l, m. Focusing particularly on tidal axisymmetric perturbations, the focus is on cases where $l = 2, m = 0$. This involves formulating and solving the equations for the fluid's Lagrangian displacement vector, ξ_i, which correlates with Y_{20}.

The total displacement vector of the system is expressed as the aggregate of contributions from each radial mode:

$$\xi^i = \sum_n a_n \xi^i_n \tag{2.73}$$

In this representation, the modes ξ_n are measured in units of length, rendering the coefficients a_n dimensionless. In scenarios devoid of the driving force from a binary companion, the fluid modes adhere to the Harmonic-oscillator equation:

$$\ddot{a}_n + \omega_n^2 a_n = 0, \tag{2.74}$$

where ω_n denotes the frequency of the nth mode. The presence of an external tidal potential modifies the equation of motion (EOM) for the internal fluid modes to that of a driven harmonic oscillator:

$$\left(-\omega^2 + \omega_n^2\right) a_n = \frac{\mathcal{E} Q_n}{M R^2}. \tag{2.75}$$

In this equation, ω represents the frequency of the external tidal field. The quadrupole associated with the nth mode, Q_n, is determined by the overlap integral

$$Q_n = -\int d^3r \, \delta\rho_n r^2. \tag{2.76}$$

The term $\delta\rho_n$ refers to the quadrupolar energy density perturbation linked with the nth fluid mode, and ΔE_n is the corresponding total mass quadrupole moment. The relationship is expressed as $Q_n = -\gamma \Delta E_n R^2$, with γ being a dimensionless number approximately equal to unity.

Focusing on the $m = 0$ modes, the driving is essentially at zero frequency, where $\omega = m\Omega$ and $\Omega = \sqrt{M/b^3}$ is the orbital frequency. Thus, Eq. (2.75) simplifies to

$$\omega_n^2 a_n = \frac{\mathcal{E} Q_n}{M R^2}. \tag{2.77}$$

Generally, for $m \neq 0$, the driving frequency can also be neglected since it is small compared to the natural frequencies of the oscillator, $\Omega^2 \ll \omega_n^2$, with $\omega_n^2 \sim 1/R^2$, and $\Omega^2 = R/b^3$, while $R^3/b^3 \ll 1$. The solution of Eq. (2.77) is given by

$$a_n = \mathcal{E} \frac{Q_n}{M \omega_n^2 R^2}. \tag{2.78}$$

The identification of the Love number is achieved by examining the asymptotic moments for a static observer at infinity, which are derived from the external metric perturbation equation (2.61), where $Q = \sum_n a_n Q_n$. By inserting $\mathcal{E}$ from Eq. (2.78) into Eq. (2.61), one obtains:

$$k_{2n} R^5 = -\frac{3}{2}\frac{Q_n}{\mathcal{E}} = -\frac{3}{2}\frac{1}{a_n}\frac{Q_n^2}{M\omega_n^2 R^2}. \tag{2.79}$$

This expression effectively links the Love number with the physical parameters of the system, providing a clearer understanding of its relationship to the external tidal forces and the internal dynamics of the object. From the decomposition of the asymptotic moment $k_2 = \sum_n a_n k_{2n}$, the Love number is deduced as

$$k_2 = -\sum_n \frac{3}{2R^5}\frac{Q_n^2}{M\omega_n^2 R^2}. \tag{2.80}$$

Redefining the results in terms of the intrinsic energy spectrum of the driven system, we define the intrinsic energy difference $\Delta E_n^{\rm int} = E_n^{\rm int} - M$ as

$$\Delta E_n^{\rm int} = \frac{1}{2} M\omega_n^2 R^2. \tag{2.81}$$

It's essential to note that the intrinsic energy difference $\Delta E_n^{\rm int}$ is solely dependent on the object's intrinsic properties and is independent of the external driving field. This concept is distinct from the energy $\Delta E_n^{\rm induced}$ pumped into mode n by the external field, expressed as

$$\Delta E_n^{\rm induced} = \frac{1}{2} M R^2 \omega_n^2 a_n^2. \tag{2.82}$$

Substituting a_n from Eq. (2.78) into Eq. (2.82) links $\Delta E_n^{\rm induced}$ to the total work done by the external tidal force:

$$\Delta E^{\rm induced} = \sum_n \Delta E_n^{\rm induced} = \frac{1}{2}\sum_n \mathcal{E} a_n Q_n = \frac{1}{2}\mathcal{E} Q. \tag{2.83}$$

Integrating Eq. (2.81) into Eq. (2.80), the final expression for the Love number is obtained:

$$k_2 = -\frac{3}{4R^5}\sum_n \frac{Q_n^2}{\Delta E_n^{\rm int}}. \tag{2.84}$$

In scenarios where the sum is predominantly influenced by the lowest energy level ($n = 1$), the Love number approximates to

$$k_2 \simeq -\frac{3}{4R^5}\frac{Q_1^2}{\Delta E_1^{\rm int}}. \tag{2.85}$$

The parameterization of Q_n can be achieved on dimensional grounds as

$$Q_n = \gamma_n \Delta E_n^{\rm int} R^2, \tag{2.86}$$

where γ_n is a dimensionless number reflecting the detailed functional form of the energy density profile of the object. Consequently,

$$k_2 = -\frac{3}{4R} \sum_n \gamma_n^2 \Delta E_n^{\rm int}. \tag{2.87}$$

Generally, it is anticipated that γ_n diminishes rapidly as n increases, indicating that higher-n modes possess more localized energy distributions and thus contribute less to the overall sum.

Given that higher-n modes have more localized energy distributions and therefore induce a smaller quadrupole moment, it is expected that the decrease in γ_n will counterbalance the increase in E_n. Hence, the Love number approximately simplifies to

$$k_2 \simeq -\frac{3}{4R} \gamma_1^2 \Delta E_1^{\rm int}. \tag{2.88}$$

This relationship can be further simplified by considering $\Delta E_1^{\rm int} \sim M\omega_1^2 R^2$ and typically $\omega_1 \sim 1/R$, leading to $k_2 \sim \gamma_1^2$.

In summary, calculating the Love number is akin to a classical linear response analysis of a set of driven harmonic oscillators subjected to an external force, particularly in scenarios where the intrinsic frequency of the oscillator significantly surpasses the driving frequency.

In the quantum scenario, the approach remains similar, but the focus shifts to the quadrupole moment of the interior modes as observed by a static observer at infinity. This perspective does not explicitly rely on the Lagrangian displacement vector or the Newtonian potential at the star's surface. These elements are instead tools for achieving a specific goal: establishing an additional boundary condition (BC) for the exterior perturbation equations. This methodology forms a bridge to the quantum Love number calculations and results within the semiclassical approximation framework. The critical factors to be determined are the energy of the lowest-lying level and the quadrupole moment associated with this level.

2.6 Relating the two methods for quantum black holes

The Love number requires only a single boundary condition (BC) at the QBH's surface.

The key physical assumptions for identifying this single BC are:

1. Both general relativity (GR) black holes (BHs) and QBHs possess a horizon.

2. Absent external perturbations, QBHs are indistinguishable from GR BHs.

3. QBHs, unlike GR BHs, exhibit geometric deformations in response to external perturbations, which manifest in their asymptotic moments. These changes in state endow QBHs with 'hair', resulting in a nonzero k_2.

4. The external metric perturbation must vanish on the deformed horizon of QBHs, just as in their classical counterparts.

5. The interior excited modes of the QBH are effectively modeled as a collection of driven harmonic oscillators, contributing to the Love number. An exact solution for Q_n is model-dependent and can be parameterized by a dimensionless number γ.

The theoretical constructs and assumptions used in this discussion lay the groundwork for interpreting how quantum black holes (QBHs) react to external disturbances. This approach aids in determining the Love number for QBHs, similar to classical systems but with unique considerations due to their quantum characteristics.

To apply these ideas to a specific case, let's examine the temporal aspect of the metric disturbance near a QBH, symbolized as δg_{tt}. We're simplifying by not considering the angular variation of this perturbation. The distance x_B symbolizes the location on the deformed surface of the QBH. We can then express the perturbation as follows:

$$-\delta g_{tt}(x_B) \approx c_1 + c_2(x_B - 1)^2. \tag{2.89}$$

When $x_B - 1$ is significantly smaller than 1, and defining ΔR as the difference $R - 2M$ where $\Delta R/2M$ is very small, we get:

$$x_B - 1 = \frac{\Delta R}{M}. \tag{2.90}$$

This expression helps in understanding the metric perturbation near the boundary of the QBH, which is vital for computing the QBH's Love number.

This formulation provides a framework for understanding the behavior of the metric perturbation near the QBH's boundary, which is crucial for calculating the Love number in the context of the QBH. To effectively apply the theoretical framework to quantum black holes (QBHs), a single additional boundary condition (BC) must be defined for the classical metric external to the QBH. This means determining an extra BC that H_{ext} must satisfy at the QBH's deformed boundary. Based on the five assumptions previously outlined, the following conditions are deduced:

1. Assumption 1 indicates that for both classical and quantum BHs, in the case of $E = 0$ (equivalently, $c_2 = 0$), the value of x_B for both BH types (x^B_{BH} and x^B_{QBH}) equals 1, and $g_{tt}(x_B) = 0$. This aligns with assumption 4.

2. From assumption 2, it is inferred that both GR BHs and QBHs possess a horizon and are indistinguishable in the absence of perturbations. However, under assumption 3, for $E \neq 0$, a physical deformation of the QBH is triggered, shifting the surface to $x_B = 1 + \delta x_B$. The specific value of δx_B is contingent on the QBH's spectrum.

3. Following assumption 1, for classical BHs, $c_1 = 0$ and $x^B_{BH} = 1$, leading to $\delta g^{tt}_{BH} \sim c_2(x_B - 1)^2 = 0$, and from Eq. (3.12), $g^{tt}_{BH}(x^B_{BH}) = 0$. Assumption 4 suggests a similar scenario for QBHs, where $g_{tt}(1 + \delta x_B) = 0$ with $x_B = 1 + \delta x_B$ representing the position of the deformed horizon.

These conditions provide a comprehensive set of criteria for the external metric of a QBH, ensuring that the theoretical model is consistent with the physical properties and behavior of both classical and quantum BHs.

The distinction between general relativity black holes (GR BHs) and quantum black holes (QBHs) hinges on the boundary condition at the BH horizon. This boundary condition eliminates the response terms (terms proportional to c_1 in Eq. (2.68)) in GR BHs, resulting in a vanishing Love number. For an observer near a classical BH, there is no perceived deviation in the horizon position; it remains fixed at $R = 2M$, and the external perturbation appears singular at this point. As per assumptions 3 and 4, the horizon of a QBH does deform, therefore, the boundary conditions on this deformed surface are regular, leading to a nonzero Love number.

Instead of imposing the condition $g_{tt}(1 + \delta x_B) = 0$, an equivalent condition is used: $\delta g_{tt}(1) = -\frac{1}{2}c_1 Y_{20}$. This approach is justified as follows: The fact that some points with $x_B = 1$ are technically within the original horizon does not impact this analysis, since the focus is on the perturbed metric far from the QBH's horizon. It's important to note that the classical metric is valid only outside the QBH horizon.

In a further examination, the expansion of H_{ext} can be expressed as follows:

$$H_{\text{ext}}(x_B) = \frac{c_1}{(x_B - 1)} + \mathcal{O}(x_B - 1) = 120k_2\frac{c_2}{x_B - 1} + \mathcal{O}(x_B - 1), \tag{2.91}$$

As a result, we obtain:

$$\delta g_{tt}(x_B) = -\frac{1}{2}c_1 + \mathcal{O}(x_B - 1) = 5k_2R^2\mathcal{E} + \mathcal{O}(x_B - 1), \tag{2.92}$$

The selection of the boundary condition (BC) is critical for defining the external solution. Since $\mathcal{E}$ (or equivalently, c_2) is specified by the BC at infinity, the fixation of

$\delta g_{tt}(x_B)$ is imperative to determine the value of c_1. In this setting, assumptions 3 and 5 are applied to choose c_1, aligning the value of k_2 with the result from the fluid calculation in Eq. (2.84):

$$c_1 = -2\delta g_{tt}(2M) = \frac{15}{2}\frac{\mathcal{E}}{(2M)^3}\sum_n \frac{Q_n^2}{\Delta E_n^{\rm int}}. \tag{2.93}$$

This method ensures uniformity in the computed Love number across various approaches, conforming to the existing theoretical structure.

Eq. (2.93) finalizes the comparison between the two classical methodologies for calculating k_2. It elucidates the relationship between the calculation of k_2, based on the spectrum of fluid modes, and the choice of boundary condition (BC) on the perturbed relativistic Einstein equations, especially in the context of a quantum black hole (QBH). If the lowest energy level significantly contributes to the sum, as expected, the approximation from Eq. (2.85) is applicable:

$$c_1 = -2\delta g_{tt}(R_B) \approx -\frac{15}{2}\frac{\mathcal{E}}{(2M)^3}\frac{Q_1^2}{\Delta E_1^{\rm int}}. \tag{2.94}$$

Furthermore, by merging Eqs. (2.67) and (2.91), we obtain:

$$-g_t(x_B) = \left(\frac{x_B-1}{x_B+1}\right)\left(1+\frac{c_1}{x_B-1}\right) + \mathcal{O}(x_B-1)^2, \tag{2.95}$$

and from the BC on the distorted surface $q_u(1+\delta x_R) = 0$, we infer that $c_1 = 1-x_R$. This insight further solidifies the understanding of the QBH's reaction to external disturbances and the computation of k_2, integrating the fluid mode spectrum with the relativistic perturbation approach.

2.7 Comparison with the Quantum Love number

In the pursuit of comparing the classical and quantum calculations of the Love number for a quantum black hole (QBH), it's noteworthy to highlight the remarkable resemblance between the classical Love number formula, as expressed in Eq. (2.84), and the quantum Love number equation presented in Eq. (2.55). By correlating the expectation values in the quantum equation with their classical counterparts, where $\langle\Psi_0|\hat{Q}_{ij}|n,2,0\rangle = Q_n$ and the internal excited energy spectrum $|\Delta E_{1,n}| = \Delta E_n^{\rm int}$, Eqs. (2.84) and (2.55) essentially become equivalent.

The quadrupole matrix element in the quantum case is calculated through the integral:

$$\left|\langle\Psi_0|\hat{Q}|n,2,0\rangle\right| = \int d^3r\, \delta\tilde{\rho}_{n,2}(r) r^2 Y_{20}\Psi_{n,2}, \tag{2.96}$$

where $\delta\tilde{\rho}_{n,2}(r)$ represents the perturbed density, and $\Psi_{n,2}$ is the wave function of the nth excited state with spherical indices $2, 0$. This integral effectively bridges the quantum mechanical representation of the quadrupole moment with its classical analog, underscoring the deep connection between the classical and quantum approaches to calculating the Love number of QBHs.

The observed correspondence between quantum and classical calculations of the Love number is a direct embodiment of the Bohr correspondence principle. This principle asserts that for macroscopic states with large quantum occupation numbers, the expectation values align with classical quantities. The states under consideration indeed embody this principle, as they are associated with large occupation numbers. For a quantum state with energy scaling as $M\omega_n^2 R^2$, the occupation number N scales in proportion to $N\hbar\omega_n \sim M\omega_n^2 R^2$, leading to $N \sim (\omega_n R)MR/\hbar \sim (\omega_n R)S_{BH}$, where S_{BH} is the Bekenstein-Hawking entropy of the QBH. This implies that $N \gg 1$, confirming the large occupation numbers of these states.

Eq. (2.93) finalizes the comparison between the quantum and classical approaches for calculating the Love number. It achieves this by clearly defining the additional boundary condition (BC) necessary for the perturbation equations that determine the external metric of a QBH. This inclusion ensures a comprehensive understanding and alignment between the classical and quantum methodologies in assessing the Love number in the context of QBHs.

In [6] a method for explicitly calculating k_2 based on only partial knowledge of the internal spectrum of an ultracompact object was shown. This object could be either a classical ultracompact star, characterized by its nonrelativistic fluid modes, or a quantum black hole (QBH), defined by its spectrum of excited states. The critical additional boundary condition (BC), which encapsulates vital information about the QBH's interior, is determined in relation to its spectrum. In both scenarios, k_2 is predominantly influenced by the first excited level or the lowest lying fluid mode and is proportional to the relative excitation energy of this level, $k_2 \sim \Delta E/M$. The proportionality coefficient is dependent on further details, specifically the ratio of the quadrupole moment of the excited level to its excitation energy ΔE.

Moreover, since the determination of k_2 boils down to identifying the ratio of two numbers, a detailed resolution of the interior is unnecessary. Information about the interior is conveyed to an external observer through deformations on the QBH's surface. This information can effectively be 'integrated out', leaving only one relevant BC.

The fact that k_2 does not vanish for a QBH represents a deviation from the no-hair property and underscores a fundamental distinction between black holes (BHs) and QBHs. For classical BHs, geometric deformations do not impact their asymptotic moments. However, for QBHs, such deformations are significant and necessitate a physical matter deformation, or equivalently, a physical response of the QBH to external perturbations. This makes it possible for an external observer to detect these effects. This emphasizes the importance of k_2 as a crucial diagnostic tool for exploring the quantum

aspects of black holes, highlighting its role in differentiating between classical BHs and QBHs and in probing the deeper quantum nature of these astrophysical objects. The concurrence between the classical and quantum approaches in calculating the Love number k_2 suggests that they are complementary methods for arriving at the same conclusion, thereby reinforcing the credibility of each calculation. This alignment not only offers a direct translation between quantum observables and classical general relativity (GR) metrics but also aligns perfectly with the Bohr correspondence principle.

However, it's important to distinguish the Love number characteristics of quantum black holes (QBHs) from those of semiclassical objects like gravastars and wormholes. Unlike QBHs, these semiclassical entities are not quantum in nature, lack an event horizon, and their unperturbed surface is located at a finite distance from the theoretical horizon, rather than at $R = 2M$. Additionally, the methodology to determine their Love number is distinct, often relying on the assumption of an infinitely thin, rigid shell made of hypothetical matter that violates both the weak and dominant energy conditions. This shell is crucial to ensure continuity from the interior to the exterior solutions. The Love number in these cases arises from the metric solution's discontinuity, a purely geometric trait, as opposed to the QBH Love number, which stems from interior matter deformation or the interaction of its ground state with higher states due to external tidal perturbations.

Chapter 3

Quantum Love number

In this chapter we will follow the work in [9] calculating the quantum Love number by using the Bohr correspondence principle, also discussed in the previous chapter.

In general, a weak external tidal field causes the emergence of small but non-zero mass (electric) and current (magnetic) moments. According to the linear response theory, these moments have a direct proportionality to the external tidal field. The most significant of these induced moments is usually the mass quadrupole. This is related to the quadrupolar tidal field E_{ab}, with the relation

$$Q_{ab} = -\frac{2}{3} k_2 R^5 E_{ab}. \tag{3.1}$$

The variable k_2 represents the dimensionless quadrupolar electric tidal Love number, while R symbolizes the radius of the object in the inspiral phase.

The value of k_2 is highly dependent on the compactness of the object, defined as C = M/R. Particularly, as C nears a black hole (BH) value, C $\to$ 1/2, a universal reduction in the Love number is observed, with it approaching zero as it reaches the BH limit. This behavior aligns with the no-hair property of BHs discussed before. The fact that k2 vanishes completely for BHs and is the largest among the dimensionless Love numbers, makes it an essential marker for identifying any departures from the classical theory of general relativity (GR) as also discussed before.

According to the Bohr correspondence principle, a quantum state corresponds to a classical BH, regardless of its size. The term "quantum black hole" (QBH) is used to denote the quantum state matching a classical BH. This UCO has a horizon and also features a discrete set of quantum mechanical energy levels. These levels can be interpreted as coherent states representing macroscopic, semiclassical QBH excitations. In its fundamental state, a QBH's external geometry is identical to Schwarzschild's geometry, however, an excited QBH displays variations from its GR depiction, potentially distinguishing it from its classical counterpart in theory.

While a classical black hole (BH) is characterized by its lack of features, known as "baldness", a quantum black hole (QBH) exhibits hair. This quantum hair is entirely

comprehensible to an external observer through the Bohr correspondence principle, this principle suggests modifications in the near-horizon geometry without the need for introducing new physical concepts. The quantum hair carries limited information, yet it could reveal significant insights into some aspects of the QBH spectrum.

It is proposed that the Love numbers form a part of this quantum hair and could be observable in principle, in particular, k2, the electric quadrupolar Love number, appears to be the most promising candidate for detection. Quantum effects in large astrophysical BHs are generally expected to be minimal, this expectation is based on the extremely small ratio of the Planck length squared to the typical curvatures, l_P^2/R_S^2. However, it is argued that for QBHs, the magnitude of quantum effects could be significantly greater.

In the study of General Relativity, the interior of a Black Hole (BH) is typically viewed as void, except for a possible singular center. The emergence of the firewall hypothesis significantly altered theories regarding Quantum Black Holes (QBHs), indicating a need for a substantial reevaluation of existing perceptions. This hypothesis, as discussed in the preceding chapter, challenges traditional views.

Neglecting the concept of remnant entities, two principal approaches have been proposed to address the firewall conundrum. The first approach suggests that the horizon vicinity is a vacuum, integrating unprecedented nonlocal physics to solve the information paradox. In this view, the freedom degrees at a distance from the horizon are similar to those within it. The singularity is often regarded as insignificant, presuming its resolution will not affect the spacetime framework near the horizon. The second approach portrays BHs as non-singular structures that prevent gravitational collapse. In this scenario, potent quantum forces distribute the singularity over a region analogous in size to the horizon. This leads to a spectrum of excitations dictated by the horizon dimensions, diverging from the Planck scale. This depiction of the BH interior necessitates a radical deviation from semiclassical gravity and incorporates unconventional matter not included in the standard model. Illustrations of this concept include Fuzzballs and the polymer model as discussed before.

A precise formulation for both electric (polar) and magnetic (axial) Love numbers (tensor) of QBHs, based on their spectral analysis was presented. The methodology echoes the process used in calculating an atom's polarizability through second-order time-independent perturbation theory. It is shown that these Love numbers are particularly influenced by the lowest energy state, meaning they do not vanish as the tidal field subtly merges the first excited state with the base state.

3.1 Bohr's correspondence principle

Before delving into the computation of quantum Love numbers, it is instructive to review the analogous method used in calculating the polarizability of an atom. Imagine an atom placed within a nearly uniform electric field, denoted as $\mathcal{E}_i$, originating from a feeble

external potential $U_{\rm ext}$, where $\mathcal{E}_i = -\frac{\partial U_{\rm ext}}{\partial x^i}$. The interaction of the atom with this field is described by the dipole moment $D = \int \rho(x')x'dV'$, summed over the atom's charge distribution. This interaction is formulated as $\hat{V}_{\rm int} = -\mathcal{E}_i\hat{D}_i$. By applying second-order time-independent perturbation theory, the induced dipole moment in the affected atom is derived. The atom's linear response to the external field is illustrated as $\langle\Psi_0|\hat{D}_i|\Psi\rangle = \alpha\mathcal{E}_i$, where $|\Psi_0\rangle = |1,0,0\rangle$ is the fundamental state of the atom, and $|\Psi\rangle$ is its first-order modification, expressed as

$$|\Psi\rangle = |\Psi_0\rangle + \sum_{n,l,m} |n,l,m\rangle \frac{\langle 1,0,0|\hat{V}_{\rm int}|n,l,m\rangle}{\Delta E_{1,n}}. \tag{3.2}$$

In this equation, α symbolizes the electric polarizability, defined by

$$\alpha = \sum_{n,|m|\leq 1} \frac{|\langle\Psi_0|\hat{D}_i|n,l=1,|m|\leq 1\rangle|^2}{\Delta E_{1,n}}. \tag{3.3}$$

The symbols l and m denote the angular quantum numbers, n the radial quantum number, and $\Delta E_{1,n} = E_1 - E_n$ the energy gap. For establishing the gravitational polarizability, or Love numbers, the electric field and dipole moment are replaced by the tidal field, alongside the corresponding mass and current moments.

In a binary system's early inspiral phase, we analyze a non-rotating quantum black hole (QBH) with mass $M_{\rm BH}$ and Schwarzschild radius R_S, paired with a mass $M_{\rm ext}$ object, orbiting circularly at radius b. At the onset of the inspiral, the BH is exposed to the slowly evolving tidal field from its companion. For $b \gg R_S$, the Newtonian potential $U_{\rm ext} = -M_{\rm ext}/|\vec{b} - \vec{x}|$ in the vicinity of the BH can be expanded as

$$U_{\rm ext}(t,\vec{x}) = U_{\rm ext}(0) + \frac{1}{2}\frac{\partial^2 U_{\rm ext}}{\partial x_i \partial x_j}\Big|_0 x_i x_j + \cdots . \tag{3.4}$$

The interaction of the QBH with the external field is characterized by the quantum trace-free symmetric mass and current multipole moments, $\hat{Q}^{(l)}$ and $\hat{S}^{(l)}$, which are the quantum analogs of classical multipoles. It is assumed that the expectation values of the mass and current moments of the BH are zero in its ground state, in line with the angular symmetry of the multipole operators and the classical no-hair theorems. Denoting the ground state of the BH by $|\Psi_0\rangle$, we have $\langle\Psi_0|\hat{Q}^{(l)}|\Psi_0\rangle = 0$ and $\langle\Psi_0|\hat{S}^{(l)}|\Psi_0\rangle = 0$. Given the slow variation of the external potential, we can consider using time independent perturbation theory.

The primary correction to the black hole (BH) ground state quadrupole can be expressed as

$$\langle\Psi_0|\hat{Q}_{kl}|\Psi\rangle = -\mathcal{E}_{ij} \sum_{n_r>1,|m|\leq 2} \frac{\langle\Psi_0|\hat{Q}_{ij}|n_r,2,m\rangle\langle n_r,2,m|\hat{Q}_{kl}|\Psi_0\rangle}{\Delta E_{1,n_r}}, \tag{3.5}$$

where $\Delta E_{1,n_r} = E_1 - E_{n_r}$. The ground state Ψ_0 is characterized by the radial number $n_r = 1$, thus the energy of the ground state is $E_1 = M_{\rm BH}$.

$$\frac{1}{2}\langle\Psi_0|\hat{Q}_{ij}|\Psi\rangle = -\lambda_2\mathcal{E}_{ij}. \tag{3.6}$$

Here, λ_2 represents the dimensional quadrupolar Love number. The dimensionless Love number k_2 is conventionally defined as $k_2 = \frac{3}{2}R^{-5}\lambda_2$. From Eq. (3.5), we have

$$k_2 = -\frac{3}{2R^5}\sum_{n_r>1,|m|<2}\frac{1}{2}\frac{|\langle\Psi_0|\hat{Q}_{ij}|n_r,2,m\rangle|^2}{|\Delta E_{1,n_r}|}. \tag{3.7}$$

Equation (3.7) establishes that, in general, a quantum mechanical object will possess a nonzero quadrupolar Love number, which is dependent exclusively on the object's quantum state and its energy spectrum. The negative value of k_2 is indicative of the fact that a black hole's (BH's) energy increases as its radius expands.

The general formulae for higher-l electric and magnetic quantum Love tensors can be derived by replicating the steps that led to Eq. (3.5). The expression for the electric Love tensor is given by:

$$k_l^E = -\sum_{n_r>1,l,|m|\le l}\frac{1}{R^{2l+1}}\frac{(2l-1)!!}{2(l-2)!}\frac{1}{l!}\frac{|\langle\Psi_0|\hat{Q}^{(l)}|n_r,l,m\rangle|^2}{\Delta E_{1,n_r}} \tag{3.8}$$

$$k_l^B = -\sum_{n>1,l,|m|\le l}\frac{1}{R^{2l+1}}\frac{(l+1)(2l-1)!!}{6(l-2)!l!}\frac{\left|\left\langle\Psi_0\left|\hat{S}^{(l)}\right|n_r,l,m\right\rangle\right|^2}{\Delta E_{1,n_r}}. \tag{3.9}$$

3.1.1 "Electric" quadrupolar Love number

The foundation for evaluating k_2 is based on Eq. (3.7). The external quadrupole tidal field aligns with the spherical harmonic Y_{20} due to the symmetry of the inspiral trajectory. The induced quadrupole mirrors this angular dependency, leading to the equation:

$$k_2 = -\frac{3}{4R^5}\sum_{n_r}\frac{|\langle\Psi_0|\hat{Q}|n_r,2,0\rangle|^2}{|\Delta E_{1,n_r}|}. \tag{3.10}$$

To calculate k_2, the discrete quantum spectrum of the QBH must be determined. Ideally, this requires solving quantum gravity equations to find the BH's spectrum. In some models, this is achievable, and is indeed the purpose of the thesis to do so, particularly in a model with energy spectrum as that of the hydrogen atom. In the case examined by the paper discussed in this chapter however, the corresponding classical wave equation is

solved, followed by the application of the Bohr correspondence principle. Initial estimates of k_2 are based on scaling arguments, which are then substantiated by calculations.

The energy spectrum of macroscopic QBH excitations, in a coherent state, follows the classical relationship $|\Delta E_{1,n_r}| \sim M_{\rm BH}\omega_{n_r}^2 R^2$, where ω_{n_r} is the frequency of mode $|n_r, 2, 0\rangle$. The scaling of the quadrupole operator's matrix element is $|\langle\Psi_0|\hat{Q}|n_r, 2, 0\rangle| \sim |\Delta E_{1,n_r}|R^2 \sim M_{\rm BH}\omega_{n_r}^2 R^4$. Hence, each term in the sum in Eq. (3.10) scales as:

$$\frac{1}{R^5}\frac{|\langle\Psi_0|\hat{Q}|n_r, 2, 0\rangle|^2}{|\Delta E_{1,n_r}|} \sim \frac{|\Delta E_{1,n_r}|}{R} \sim \frac{|\Delta E_{1,n_r}|}{M_{\rm BH}} \sim \omega_{n_r}^2 R^2. \tag{3.11}$$

This semiclassical approach is validated by observing that the excited energy levels' occupation numbers N scale as $N\hbar\omega_{n_r} \sim M_{\rm BH}\omega_{n_r}^2 R^2$, so $N \sim (\omega_{n_r} R)\, S_{\rm BH} \gg 1$. Furthermore, both scaling arguments and explicit computations indicate that the contributions to k_2 in Eq. (3.10) from states beyond the first excited state are minor, allowing for an approximation of the sum over n_r by the first excited state's contribution. This pattern is typical in many quantum systems.

Moreover, since all terms in the sum are positive, the approximate value of the magnitude of k_2 tends to be an underestimate. It is then reasonable to approximate the sum by considering only the contribution from the first excited state. Combining the two scaling arguments, we arrive at an estimate for k_2:

$$k_2 = -\frac{3}{4R^5}\frac{\left|\left\langle\Psi_0|\hat{Q}|2, 2, 0\right\rangle\right|^2}{|\Delta E_{1,2}|} \sim -\frac{|\Delta E_{1,2}|}{M_{\rm BH}} \sim -\omega_2^2 R^2 \tag{3.12}$$

We now shift our focus to a detailed evaluation of k_2, aiming to determine the numerical factor of order unity in Eq. (3.12). It's important to note that the estimate in Eq. (3.12) holds true regardless of the specific model used. The model we examine here is chosen for its simplicity and the ability to analytically calculate numerical factors. This model will later be used to parameterize the Love number in terms of the single parameter g^2 and assess its detectability based on the estimate in Eq. (3.12).

Given the strong coupling of gravity within a black hole's (BH's) interior, a semiclassical geometric description using curved spacetime is not feasible. Instead, gravity is represented as an inertial force in flat space, an approach permitted by Einstein's equivalence principle. The specific nature of the interior excitations is deemed irrelevant, as is the distinction between the two gravitational descriptions. The key factor is that these excitations are macroscopic, horizon-scale, justifying the application of the Bohr principle.

The internal structure of the quantum black hole (QBH) can be conceptually viewed as a fluid supporting pulsating modes, similar to those in a relativistic star. These fluid modes coexist with the standard spacetime modes of the exterior. The perturbations are categorized into two types: fluid modes and spacetime modes. Due to their low

sound velocity and the QBH's compactness, the fluid modes are effectively isolated from spacetime perturbations, as per the Cowling approximation.

For boundary conditions (BCs), spherical symmetry dictates fully reflecting BCs at the QBH's center. The QBH also possesses an outer surface that mimics a classical BH horizon in the classical limit. Here, the internal fluid modes are decoupled from the exterior, leading to the conclusion that a perfectly reflecting outer surface is the appropriate BC. In scenarios where quantum effects are minimal, the outer surface becomes partially transparent, leading to imperfect reflection. However, quantitative analysis shows that both BCs yield almost identical spectra. Given the simplicity of analysis with the former BC, it is chosen for the outer surface to determine the spectrum of normal modes, rather than quasinormal modes.

We deduce that the classical equation to be solved is the Laplace equation, $\vec{\nabla}^2\Psi_2(r) = 0$, with the general boundary condition (BC) $\Psi_2|_{r=0} = 0$, and $\Psi_{0,2}|_{r=R} = 0$. The solution to the Laplace equation is given by

$$\Psi_2(r) = N_2 j_2(qr) Y_{20}(\theta, \phi), \tag{3.13}$$

where j_2 is the spherical Bessel function, Y_{20} is the (real) spherical harmonic function with $l = 2$, $m = 0$, and N_2 is a normalization factor, which will be determined subsequently.

The normalization factor will be ascertained later. In this scenario, the boundary condition (BC) permits only discrete values for the magnitude of the wave number q,

$$J_l'(qR) = 0, \tag{3.14}$$

which is closely approximated by

$$q_{n_r} = \left(n_r - \frac{1}{2}\right)\frac{\pi}{R}, \quad n_r = 3, 4, \ldots, \tag{3.15}$$

except for $n_r = 2$, where the value is slightly lower,

$$q_2 = 1.06\frac{\pi}{R}. \tag{3.16}$$

Condition (3.15) can also be interpreted as a reflection of the Bohr quantization condition in the corresponding quantum black hole (QBH). Replacing P with $\hbar q$, we obtain

$$PR = \hbar\pi\left(n_r - \frac{1}{2}\right). \tag{3.17}$$

Our next step is to compute $|\Delta E_{1,2}|$ and $|\langle\Psi_0|\hat{Q}|\Psi_2, 2, 0\rangle|$ using the solution $\Psi_{2,2} = N_{2,2} j_2(q_2 r) Y_{2,0}$ with the aforementioned wave number. Initially, considering the classical waves are non-relativistic,

$$|\Delta E_{1,2}| = \frac{1}{2} M_{\rm BH}\omega_0^2 R^2 = \frac{1}{2} M_{\rm BH} q_2^2 R^2. \tag{3.18}$$

Here, we introduce a parametrized dispersion relation $\omega_0^2 = g^2 q_2^2$, where $g^2 \ll 1$ is the key parameter determining the energy of the first excited level in our model.

To assess the expectation value $|\langle\Psi_0|\hat{Q}|\Psi_2, 2, 0\rangle|$ as in Eq. (3.12), a more detailed calculation is required. Initially, we need the general expression for the excitation energies for $n_r \geq 3$, The excitation energy for each mode is given by

$$|\Delta E_{1,n_r}| = \frac{1}{2} g^2 M_{\rm BH} \pi^2 \left(n_r - \frac{1}{2}\right)^2, \tag{3.19}$$

where we have incorporated any additional n_r-independent factors into g^2 and assumed that the dispersion relation holds true for all modes. The excitation energy must be significantly smaller than the BH mass, $|\Delta E_{1,n_r}| \ll M_{\rm BH}$.

To continue, the classical counterpart of the matrix element $|\langle\Psi_0|\hat{Q}|2, 2, 0\rangle|$ is represented by

$$|\langle\Psi_0|\hat{Q}|2, 2, 0\rangle| \leftrightarrow \int r^2 {\rm d}r \, {\rm d}\Omega_2 \, \Delta\rho_{2,2}(r) \, r^2 Y_{20} \Psi_{2,2}. \tag{3.20}$$

The evaluation of this quantity entails the computation of the effective energy density within the first excited state, $\Delta p_2(r)$, by means of the following comparative analysis. Initially,

$$|\Delta E_{1,n}| = \int r^2 dr \Delta p_2(r). \tag{3.21}$$

Conversely, when considering the lowest order in g^2, the energy $|\Delta E_{1,n}|$ shows a direct proportionality to ω_n^2,

$$|\Delta E_{1,n_r}| = \int r^2 dr d\Omega_2 \, |\Psi_{2,n_r}|^2 \, \omega_{n_r}^2 = |\mathcal{N}_{2,n_r}|^2 \int_0^R r^2 dr j_2^2 \left(\frac{\omega_{n_r}}{g} r\right) \omega_{n_r}^2, \tag{3.22}$$

where the authors have utilized specified equations and completed the angular integration. In comparing the two stated forms of $|\Delta E_{1,n}|$, it is determined that

$$\Delta\rho(r)_{2,n_r}(r) = \frac{|\Delta E_{1,n_r}|}{I_{2,n_r}} j_2^2 \left(\frac{\omega_{n_r}}{g} r\right) \tag{3.23}$$

and

$$|\mathcal{N}_{2,n_r}|^2 = \frac{|\Delta E_{1,n_r}|}{\omega_{n_r}^2 I_{2,n_r}} \tag{3.24}$$

where

$$I_{2,n_r} = \frac{R^3}{\pi^3 \left(n_r - \frac{1}{2}\right)^3} \int_0^{\pi\left(n_r - \frac{1}{2}\right)} y^2 dy j_2^2(y) \tag{3.25}$$

The substitution of the prior equation into a preceding expression yields:

$$\begin{aligned}\left|\left\langle \Psi_0|\hat{Q}|n_r,2,0\right\rangle\right| &\leftrightarrow \int r^2 dr d\Omega_2 \frac{|\Delta E_{1,n_r}|}{I_{2,n_r}} j_2^3\left(\frac{\omega_{n_r}}{g}r\right)(Y_{20})^2 \\ &= |\Delta E_{1,n_r}|\,\mathcal{N}_{2,n_r}\frac{I_{4,n_r}}{I_{2,n_r}},\end{aligned} \tag{3.26}$$

where

$$I_{4,n_r} = \frac{R^5}{\pi^5\left(n_r-\frac{1}{2}\right)^5}\int_0^{\pi\left(n_r-\frac{1}{2}\right)} dy y^4 j_2^3(y) \tag{3.27}$$

In the analysis that follows, the sum of terms with $n \geq 3$ is derived from a previous equation as

$$\begin{aligned}&\sum_{n_r=3}\frac{|\Delta E_{1,n_r}|^2}{\omega_{n_r}^2}\frac{I_{4,n_r}^2}{I_{2,n_r}^3} \\ &\quad= \frac{1}{4}g^2 M_{\rm BH}^2 R^3 \sum_{n_r=3}\pi\left(n_r-\frac{1}{2}\right)\left(\tilde{I}_{4,n_r}\right)^2\left(\tilde{I}_{2,n_r}\right)^{-3},\end{aligned} \tag{3.28}$$

where the energy spectrum and the integral $I_{2,n} = \int_0^R y^2 dy j_0^2(y)$, which linearly scales with $\pi(n-\frac{1}{2})$, and $I_{4,n}$, approximately constant, are considered. The authors note that even and odd powers of the spherical Bessel function scale differently, resulting in a sum scale of $1/(n-\frac{1}{2})^2$, where the terms associated with odd n are markedly smaller than those with even n. The dominant term is for $n=2$, and the subsequent significant term is for $n=4$, which is roughly one-fifth the magnitude of the former.

With the known values of $|\Delta E_{1,2}|$ and $\left|\left\langle \Psi_0|\hat{Q}|2,2,0\right\rangle\right|$, their substitution into an earlier equation yields

$$\begin{aligned}k_2 &= -\frac{3}{16}\frac{1}{q_2 R}\frac{M_{\rm BH}^2}{R^2}\frac{\tilde{J}_4^2}{\tilde{J}_2^3}\omega_2^2 R^2 \\ &= -\frac{3}{16}q_2 R\frac{M_{\rm BH}^2}{R^2}\frac{\tilde{J}_4^2}{\tilde{J}_2^3}g^2,\end{aligned} \tag{3.29}$$

Taking into account analytically evaluated integrals j_2 and j_4, and by setting $M_{BH}/R = 1/2$, the derived final results are

$$k_2 = -0.09 g^2 R^2 = -0.18\frac{|\Delta E_{1,2}|}{M_{BH}} = -0.09 g^2. \tag{3.30}$$

Proceeding with the anticipated scaling of k_2 as $\omega_2^2 R^2$, the computed k_2 value are to be compared to those characterizing other compact objects. It is observed that for neutron stars, k_2 is not only positive but also significantly greater in magnitude than the computed value. In the context of exotic UCOs, previous studies have indicated a

universal logarithmic dependence. These studies posited modifications at the UCO outer surface, $R = 2M(1+\epsilon)$, leading to the conclusion that $k_2 \sim 1/|\ln\epsilon|$ and is negative. Furthermore, the real part of the frequency for spacetime modes associated with UCOs, specifically for the $n = 2$ mode, is $\omega_{2,UCO} \sim 1/|\ln\epsilon|$. Within the framework of the Black Hole area quantization model, the frequency ω_n is defined as $\alpha_n/16\pi R$, with α being a dimensionless coefficient, typically of order unity. Applying the semiclassical analysis, it is found that

$$k_2 \approx \frac{3}{16}\left(\frac{\alpha}{8\pi}\right)^2. \tag{3.31}$$

Chapter 4

The Hydrogen Model of the Black Hole

In this chapter we will follow the work of professor Casadio Roberto in "A quantum bound on compactness" [5] showing a model of the interior of a black hole consisting of dust particles, this model shares the same energy level structure as the hydrogen atom making it a reasonable candidate for the further computation of the "electric" quadrupolar Love number discussed earlier, that is, it provides a quantum theory of the energy spectrum for a direct computation of the quadrupolar Love number instead of relying on the Bohr correspondence principle. We will modify the model by adding an angular component to it making it eligible for computing the k2 Love number with the formula presented earlier.

4.0.1 A brief overview on minisuperspaces

Minisuperspace is a concept in quantum cosmology that simplifies the study of the universe's structure at a quantum level. In this context, the Friedman-Lemaître metric, a solution to Einstein's field equations in a homogeneous and isotropic universe, is often used as an example. The metric is given by:

$$ds^2 = -dt^2 + a(t)^2 \left[\frac{dr^2}{1 - kr^2} + r^2(d\theta^2 + \sin^2\theta \, d\phi^2) \right], \tag{4.1}$$

where $a(t)$ is the scale factor and k represents the curvature of space. This approach reduces the infinite degrees of freedom in the full superspace to a finite, manageable number by focusing on a subset of metrics and matter fields configurations. This simplification makes the complex Wheeler-DeWitt equation, which describes the quantum state of the entire universe, more tractable [11, 12]. The minisuperspace models often consider only homogeneous and isotropic metrics, thus ignoring spatial inhomogeneities and anisotropies, which are essential in the early universe but can be neglected at larger

scales. The idea is to capture the most significant features of the universe's quantum behavior while avoiding the computational infeasibility of a full quantum gravity treatment. Minisuperspace models have been instrumental in exploring various aspects of quantum cosmology, such as singularity resolution, quantum potentials, and the early universe dynamics [13, 14].

4.0.2 Hydrogen model for gravitational collapse

The concept that quantum gravity might address the singularity predicted by General Relativity during gravitational collapse has been frequently discussed. This analysis examines a basic quantum model of a dust ball in gravitational collapse. Under these conditions, where gravity is the only force acting on the dust, the dust ball's areal radius R follows a radial geodesic in the external Schwarzschild spacetime. This spacetime is represented by the metric

$$ds^2 = -\left(1 - \frac{2G_N M}{r}\right) dt^2 + \left(1 - \frac{2G_N M}{r}\right)^{-1} dr^2 + r^2 d\Omega^2, \tag{4.2}$$

where M stands for the Arnowitt–Deser–Misner (ADM) mass of the dust.

Drawing an analogy with quantum mechanics in a hydrogen atom, where the electron's position relative to the nucleus is quantized, this study quantizes the radius R of the dust ball. Hence, the radial geodesic equation evolves into a time-independent Schrödinger equation, similar to a particle in a Newtonian potential. Notably, quantum states with widths much smaller than the gravitational radius $RH = 2G_N M$ are considered physically implausible. This parallels how quantum mechanics resolves the classical ultraviolet (UV) catastrophe in a hydrogen atom. However, this model distinctively introduces a lower bound on the energy spectrum determined by the mass M, a feature absent in the Newtonian model. This suggests that the quantum properties of black holes as extended entities might be due to the non-linear nature of gravitational interactions, as depicted in General Relativity.

Let's now focus on a self-gravitating dust ball characterized by radius R and ADM mass M . Within General Relativity's framework, the dust ball's surface is constrained to follow a radial geodesic in the Schwarzschild spacetime. Its areal radius, denoted as $R = R(\tau)$, must conform to the equation

$$\left(\frac{dR}{d\tau}\right)^2 + 1 - \frac{2G_N M}{R} = \frac{E^2}{M^2}, \tag{4.3}$$

where τ represents the proper time and $E < M$ denotes the conserved energy of a bounded trajectory. This equation can be rephrased as

$$H \equiv \frac{P^2}{2M} - \frac{G_N M^2}{R} = \frac{M}{2}\left(\frac{E^2}{M^2} - 1\right) \equiv E, \tag{4.4}$$

with $P = M\frac{dR}{d\tau}$ being the momentum. Eq. (4.4) is akin to the energy conservation equation in Newtonian physics, serving as the mass-shell condition for the dust ball and reflecting the Hamiltonian constraint in General Relativity for dust.

A simple quantization method can be applied to the above equation, introducing the momentum operator $\hat{P} = -i\hbar\frac{\partial}{\partial R}$. This implies that the ball's radius R is subject to an uncertainty principle, derived from the canonical commutator, stated as

$$[\hat{R}, \hat{P}] = i\hbar \quad \Rightarrow \quad \Delta R \Delta P \gtrsim \hbar = \ell_{\rm p} m_{\rm p} \tag{4.5}$$

where ΔO is defined as $\sqrt{\langle \hat{O}^2 \rangle - \langle \hat{O} \rangle^2}$ for $\hat{O} = \hat{R}$ or $\hat{P}$. Expectation values are determined over wavefunctions $\psi = \psi(R)$ that fulfill $\hat{H}\psi = E\psi$, the time-independent Schrödinger equation for a gravitational (Newtonian) atom. The energy spectrum features eigenstates

$$\Psi_n \simeq \sqrt{\frac{M^9}{\pi n^5 \ell_{\rm p}^3 m_{\rm p}^9}} e^{-\frac{M^3 r}{n m^3 \ell_{\rm p}}} L_{n-1}^1 \left(\frac{2M^3 r}{n m_{\rm p}^3 \ell_{\rm p}} \right). \tag{4.6}$$

where $n \geq 1$ is an integer, and L_1^{n-1} are the generalized Laguerre polynomials (for zero angular momentum). The corresponding eigenvalues are

$$\frac{\mathcal{E}_n}{M} \simeq -\frac{G_{\rm N}^2 M^4}{2\hbar^2 n^2} = -\frac{1}{2n^2}\left(\frac{M}{m_{\rm p}}\right)^4 = \frac{1}{2}\left(\frac{E_n^2}{M^2} - 1\right) \tag{4.7}$$

and it is deduced that

$$R_n \equiv \langle \Psi_n | R | \Psi_n \rangle \simeq \frac{\hbar^2 n^2}{G_{\rm N} M^3} = n^2 \ell_{\rm p} \left(\frac{m_{\rm p}}{M}\right)^3. \tag{4.8}$$

Initially, it might seem that the spectrum includes states ψ_n with infinitesimally narrow widths, particularly for macroscopic objects like stars, where $M \gg m_p$. The ground state R_1 could be approximated by

$$\ell_{\rm p} \left(m_{\rm p}/M\right)^3 \ll \ell_{\rm p}$$

The ground state energy density is of the order

$$M/R_1^3 \sim \left(M^{10}/m_{\rm p}^9\right) \ell_{\rm p}^{-3}$$

, which, while extremely high, does not reach the infinite energy density characteristic of classical singularities.

When Equation (4.7) is evaluated, it gives a bound:

$$0 \leq \frac{E_n^2}{M^2} \approx 1 - \frac{1}{n^2}\left(\frac{M}{m_{\rm p}}\right)^4 \tag{4.9}$$

which is essentially equivalent to

$$\mathcal{E} \geq -\frac{M}{2} \tag{4.10}$$

as per Equation (4.4). From this, it is deduced that acceptable quantum states, denoted by n, must fulfill the condition

$$n \geq N_M \approx \left(\frac{M}{m_{\rm p}}\right)^2 \tag{4.11}$$

This leads to the conclusion that

$$R_n \geq R_{NM} \approx R_H \tag{4.12}$$

This boundary condition implies the upper bound

$$\frac{G_{\rm N} M}{R_n} \lesssim 1 \tag{4.13}$$

highlighting a significant constraint on the system.

Furthermore, the lower bounds for the Hamiltonian eigenvalues are established as

$$\mathcal{E}_n \geq \mathcal{E}_{N_M} \approx -\frac{M}{2} \tag{4.14}$$

which corresponds in turn to

$$E_n^2 \geq E_{N_M}^2 \approx 0 \tag{4.15}$$

In the context of a semiclassical state representing a collapsing dust ball, such a state must be expressed as a superposition of states n with $n \geq N_M$. Given the quantum bound mentioned earlier (Eq. 4.13), this implies that for any dust ball, the compactness parameter $\frac{G_N M}{R}$ should be approximately 1 or less. It's crucial to emphasize that this result is an approximation, valid up to a factor of the order of one. More precise estimates might be possible with more comprehensive and realistic models, though it seems unlikely that these refinements would significantly reduce the minimum size from a fraction of R_H to the Planck length scale $\ell_{\rm p}$.

The current model, termed the 'minisuperspace' description, only incorporates the observable R. Therefore, from the wavefunction $\psi = \psi(R)$, one can deduce information such as the expectation value of R and the probability that the dust ball resides within its gravitational radius, expressed as

$$P(R \leq R_H) \equiv \int_0^{R_H} P(R) dR = 4\pi \int_0^{R_H} |\psi(R)|^2 R^2 dR, \tag{4.16}$$

This probability can be interpreted as the likelihood of the dust ball being a black hole, assuming the mass M is a fixed parameter.

Specifically, for the ground state, the wavefunction is given by

$$\Psi = \Psi_{N_M} \simeq \sqrt{\frac{m_{\rm p}}{\pi \ell_{\rm p}^3 M}} e^{-\frac{Mr}{m_{\rm p}\ell_{\rm p}}} L^1_{\frac{M^2}{m_{\rm p}^2}-1}\left(\frac{2Mr}{m_{\rm p}\ell_{\rm p}}\right) \tag{4.17}$$

This wavefunction is crucial for understanding the quantum mechanical properties of the self-gravitating dust ball, particularly in the context of gravitational collapse and black hole formation.

For small values of the ADM mass M, significantly less than the Planck mass m_p, the probability density P exhibits a pronounced peak just below the gravitational radius R_H.

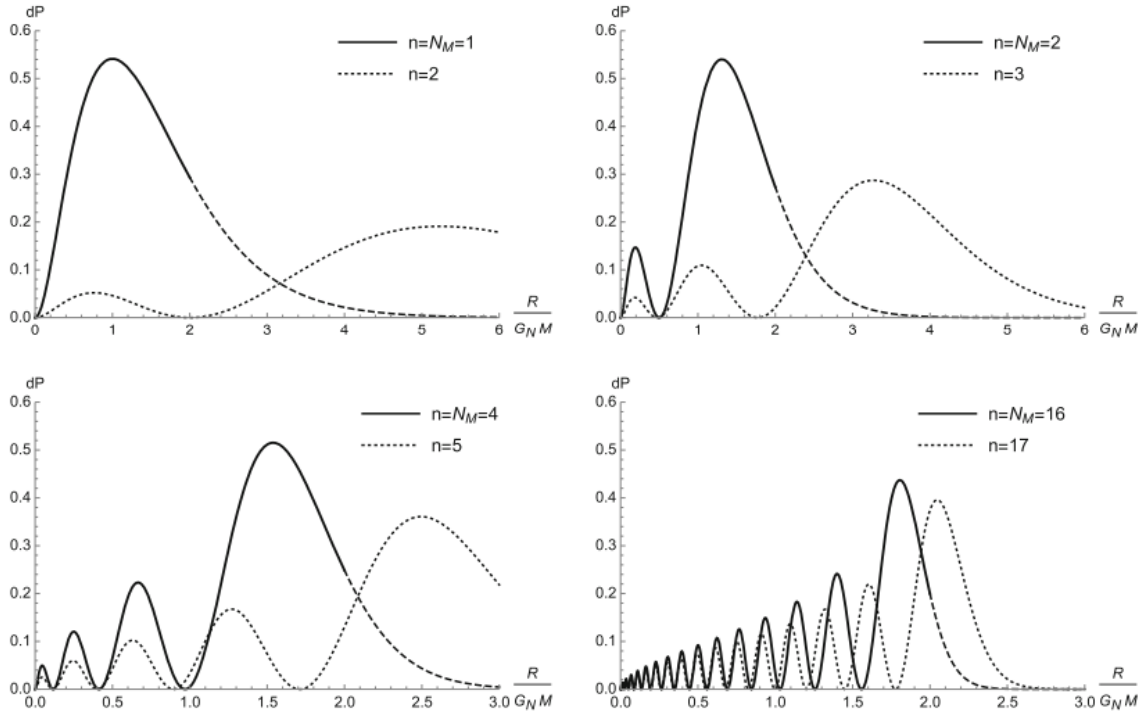

Figure 4.1: Illustration of the probability density $P = P(R)$. Panel (a) shows the ground state ($n = N_M = \frac{M^2}{m_p^2}$) with solid and dashed lines indicating the regions inside and outside the gravitational radius $R_H = 2G_N M$, respectively. Panel (b) depicts the first excited state ($n = N_M + 1$) represented by a dotted line. From [5].

where $P_{N_M}(R \leq R_H)$ closely approaches unity:

$$P_{N_M}(R \leq R_H) \approx 1. \tag{4.18}$$

Furthermore, the peak's width is inversely proportional to the mass M:

$$\Delta R_{N_M} \sim \frac{R_{N_M}}{N_M} \sim \ell_{\rm p}\frac{m_{\rm p}}{M} \tag{4.19}$$

This narrowness in ΔR_{N_M} suggests that the radius for a significantly massive dust ball behaves analogously to a classical radius.

The first excited state tends to converge towards the ground state as M increases, implying that the probability $P_n(R \leq R_H)$ approaches unity for states where $n \geq N_M$. This suggests that sizable astrophysical black holes of a given mass M might not be necessarily in the ground state $n = N_M$. In particular, when $n \geq N_M$, the increment of the Hamiltonian H, as defined earlier, can be approximated as:

$$\delta H \equiv |\mathcal{E}_{n+1} - \mathcal{E}_n| \simeq m_{\rm p} \frac{m_{\rm p}}{M} \tag{4.20}$$

Therefore $\delta H \sim m_{\rm p} \left(\Delta R_{N_M}/\ell_{\rm p}\right) \ll m_{\rm p}$ for objects with $M \gg m_{\rm p}$

Moreover the energy differential δE between adjacent quantum states is on the order of the Planck mass:

$$\delta E \approx m_p. \tag{4.21}$$

In this investigation, the General Relativistic approach to gravity is shown to establish an upper limit on the compactness of a quantum theoretical dust ball. This bound is a consequence of the nonlinearity inherent in General Relativity, distinct from the Newtonian theory where the entire spectrum of states $n \geq 1$ would be considered valid. The compactness limit thus emerges from these relativistic considerations.

In the realm of quantum mechanics, when applied to gravitational scenarios, conclusions similar to those of General Relativity are reached. Particularly noteworthy are findings regarding the probability of a black hole's formation and the uncertainty in its radius. The ground state of a self-gravitating object, modeled as an extended many-body system, has a significant occupation number, which can lead to thermal population of the first excited states, reminiscent of Hawking radiation.

This approach also aligns with the scaling relations used in the corpuscular description of black holes. The state of minimum energy correlates with a principal quantum number indicative of the number of soft gravitons in a coherent state, which in turn is linked to the quantization of the black hole's ADM mass. The typical energy of particles emitted during Hawking evaporation is related to the depletion of the quantum state of gravity, as described in this corpuscular picture.

Further, the wavefunction $\psi_{N_M} = \psi_{N_G}$ is identified as the "non-perturbative ground state" for massive self-gravitating objects, closely resembling a classical black hole, this is consistent with the idea that a static gravitational field is entirely determined by its source and lacks independent degrees of freedom in a static system. The significant deviation of the quantum state of a macroscopic self-gravitating system from the quantum gravity vacuum state is quantitatively represented by the relationship $N_M \sim N_G \sim M^2$. The emergence of this ground state when the ADM energy follows (4.11) indicates a form of classicalization, contributing to the ultraviolet self-completeness of gravity.

While the quantum states corresponding to classical singularities appear to be absent from the spectrum, determining a more precise maximum compactness value is

crucial for understanding quantum deviations from the Schwarzschild geometry. An explicit description of the exterior spacetime and its interaction with signals detectable by our instruments is needed for practical applications. The potential quantum deviations caused by the finite size of the self-gravitating system suggest a need for a more unified description of the quantum states of collapsing objects and the quantum gravitational potential.

4.0.3 Perturbed solution

we will slightly modify the model previously presented by generalizing its solution to a rotating model containing spherical harmonics by means of an approximation, we will infact renormalize the wavefunction presented previously making it eligible for the computation of the quadrupolar Love number discussed in the chapter "Quantum Love number".

We start with the wave function $\psi_{n,l}(r,\theta)$ given by:

$$\psi_{n,l}(r,\theta) = \sqrt{\frac{(2M^3/(nm_p^3 l_p))^3 (n-l-1)!}{2n(n+l)!}} \left(\frac{2rM^3}{nm_p^3 l_p}\right)^l \exp\left(-\frac{M^3 r}{nm_p^3 l_p}\right) L_{n-l-1}^{(2l+1)}\left(\frac{2rM^3}{nm_p^3 l_p}\right) Y_{l,0}(\theta,\phi) \tag{4.22}$$

This expression can be obtained by normalizing the ansatz:

$$\tilde{\psi}_{n,l}(r,\theta) \sim \left(\frac{2rM^3}{nm_p^3 l_p}\right)^l \exp\left(-\frac{M^3 r}{nm_p^3 l_p}\right) L_{n-l-1}^{(2l+1)}\left(\frac{2rM^3}{nm_p^3 l_p}\right) Y_{l,0}(\theta,\phi) \tag{4.23}$$

what was done was adding a term (equal to the argument of the Laguerre as it happens for the hydrogen atom solution) elevated to the quantum number l, it can indeed be shown that by taking l=0 the results coincide how it is expected to happen.

$$\Psi_n \simeq \sqrt{\frac{M^9}{\pi n^5 \ell_{\rm p}^3 m_{\rm p}^9}} e^{-\frac{M^3 r}{nm_{\rm p}^3 \ell_{\rm p}}} L_{n-1}^1\left(\frac{2M^3 r}{nm_{\rm p}^3 \ell_{\rm p}}\right) \tag{4.24}$$

The matrix element we are interested in calculating is:

$$\langle \psi_{n,0,0} | \hat{Q} | \psi_{n',2,m} \rangle = \int R_{n,0}^*(r) R_{n',2}(r) r^4 dr \int Y_{0,0}^*(\theta,\phi) Y_{2,m}(\theta,\phi) Y_{2,m}(\theta,\phi) \sin(\theta) d\theta d\phi. \tag{4.25}$$

In light of the orthogonality relations for spherical harmonics, as expressed by the equation

$$\int_0^{2\pi} \int_0^{\pi} Y_\ell^m(\theta,\phi) Y_{\ell'}^{m'*}(\theta,\phi) \sin\theta \, d\theta \, d\phi = \delta_{\ell\ell'} \delta_{mm'}, \tag{4.26}$$

it becomes necessary to define $\hat{Q} = r^2 Y_{20}(\theta,\phi)$. This choice ensures that $\hat{Q}$ is its own complex conjugate, a condition stemming from the non-existence of an $e^{im\phi}$ component,

and guarantees a non-zero integral when involving spherical harmonics. This formulation simplifies the problem to evaluating $\langle n, 0|r^2|n', 2\rangle$.

To compute the matrix element $\langle n, 0|r^2|n', 2\rangle$, we focus on the radial part of the wave function. By substituting $t = \frac{M^3 r}{m_p^3 l_p}$ and $dr = \frac{m_p^3 l_p}{M^3} dt$, we arrive at the integral:

$$\langle n, 0|r^2|n', 2\rangle = C \int_0^\infty t^6 e^{-t\left(\frac{1}{n}+\frac{1}{n'}\right)} L_{n-1}^{(1)}\left(\frac{2t}{n}\right) L_{n'-3}^{(5)}\left(\frac{2t}{n'}\right) dt \tag{4.27}$$

where C is given by:

$$C = \left(\frac{m_p^3 l_p}{M^3}\right)^5 \left(\frac{2}{n'}\right)^2 \left(\frac{2M^3}{m_p^3 l_p}\right)^3 \sqrt{\frac{1}{n^3 n'^3} \frac{(n-1)!(n'-3)!}{4nn'n!(n'+2)!}} \tag{4.28}$$

Computing the integral (computation method and code in the appendix) yields

$$k2 = -\frac{4.77285410 \times 10^{31} 1 p^4 m p^{16}}{M^{17} R^5} \tag{4.29}$$

The computation is done assuming a ground state with n reasonably high although not realistically high for computational reasons.

Chapter 5

Conclusions

In this thesis, we explored the quantum dynamics of black holes, with a particular focus on paving the way for further exploration through the lens of the quadrupolar Love number. Drawing upon the foundational theories and methodologies presented in the works of Ram Brustein and Yotam Sherf, we adopted a perturbative approach rooted in quantum mechanics. This approach was further refined by incorporating a complete quantum model for the energy spectrum of quantum black holes (QBHs), inspired by the well-studied hydrogen atom. This choice was motivated by the use of this model in [5] but also by its simplicity and the depth of existing research on its dynamics, allowing for an elegant application to the quantum description of black holes.

The formulation developed and exposed in this thesis for calculating the Love number has yielded a formula that enables, at least theoretically, the analytical determination of this critical quantity. The computational challenges posed by the high principal quantum number inherent in the model did not deter us from achieving a reasonable estimation of k_2 by considering a reasonably high number for the ground state. Consistent with findings from the literature, our results also indicated that the Love number for QBHs is negative, reinforcing the notion that quantum mechanical effects play a significant role in the physical characteristics of black holes.

This work considered the implications of existing research, particularly the insightful revelations about QBHs. We noted that unlike classical black holes, which adhere to the no-hair theorem and exhibit vanishing Love numbers, QBHs manifest non-zero Love numbers. This distinction underscores a fundamental quantum mechanical influence on the black hole's response to external perturbations, offering a window into their internal dynamics, moreover, the methodological advancements allowing for the Love number's calculation based on partial knowledge of the internal spectrum represent a significant leap forward, providing a streamlined approach to probing the quantum aspects of black holes.

The exploration however acknowledged the inherent limitations of its methodological choices, especially the approximation made in determining the wavefunction. The

reliance on perturbed solutions based on the minisuperspace model discussed based on the Schwartzschild metric, while practical, suggests a simplified view that might miss the intricacies captured by a more thorough treatment, such as one that incorporates the effects of rotation from the beginning, for example using a model based on the Kerr metric.

In synthesizing the findings from the articles reviewed and the research conducted, this thesis contributes to a deeper understanding of black holes from both a quantum mechanical and gravitational perspective. The negative Love numbers obtained for QBHs not only challenge traditional views established by the no-hair theorem but also highlight the nuanced interplay between quantum mechanics and general relativity in describing these astrophysical objects. The realization that Love numbers can serve as a diagnostic tool for differentiating between classical and quantum black holes opens new avenues for future experimental and theoretical work, particularly in the context of detecting these effects through forthcoming astronomical observations such as LISA.

Looking forward, the thesis underscores the need for and potential of developing more sophisticated models that can more accurately capture the spectrum of QBHs. Such advancements are crucial for unraveling the quantum gravitational dynamics of black holes.

Appendix A

The constants for the integral are identified as follows:

- $\alpha = 7$
- $a = \frac{2}{n}$
- $b = \frac{2}{n'}$
- $p = \frac{1}{n'} + \frac{1}{n}$
- $m = n - 1$
- $n = n' - 3$
- $\lambda = 1$
- $\beta = 5$

Using the integral formula http://functions.wolfram.com/05.08.21.0009.01 , we substitute these constants to obtain an expression involving Pochhammer symbols:

$$\begin{aligned}
&\int_0^\infty \frac{t^{(\alpha-1)}\text{LaguerreL}[m,\lambda,at]\text{LaguerreL}[n,\beta,bt]}{e^{(pt)}}dt \\
&= \frac{(\Gamma[\alpha](\lambda+1)_m(\beta+1)_n)}{(p^\alpha(m!n!))} \\
&\quad \times \sum_{j=0}^{m}\left[\frac{((-m)_j(\alpha)_j)}{((\lambda+1)_j j!)}\left(\frac{a}{p}\right)^j\right. \\
&\quad\quad \left.\times \sum_{k=0}^{n}\left[\frac{((-n)_k(\alpha+j)_k)}{((\beta+1)_k k!)}\left(\frac{b}{p}\right)^k\right]\right]
\end{aligned} \tag{A.1}$$

Where the Pochhammer symbol is defined as:

$$(x)_n \equiv \frac{\Gamma(x+n)}{\Gamma(x)} = x(x+1)\cdots(x+n-1) \tag{A.2}$$

Substituting the identified constants ($\alpha = 7$, $a = \frac{2}{n}$, $b = \frac{2}{n'}$, $p = \frac{1}{n'} + \frac{1}{n}$, $m = n-1$, $n = n'-3$, $\lambda = 1$, $\beta = 5$), the expression becomes:

$$\begin{aligned} &= \frac{(\Gamma[7](2)_{n-1}(6)_{n'-3})}{\left(\left(\frac{1}{n'}+\frac{1}{n}\right)^7((n-1)!(n'-3)!)\right)} \\ &\quad \times \sum_{j=0}^{n-1}\left[\frac{((1-n)_j(7)_j)}{((2)_j j!)}\left(\frac{\frac{2}{n}}{\frac{1}{n'}+\frac{1}{n}}\right)^j\right. \\ &\quad \left. \times \sum_{k=0}^{n'-3}\left[\frac{((3-n')_k(7+j)_k)}{((6)_k k!)}\left(\frac{\frac{2}{n'}}{\frac{1}{n'}+\frac{1}{n}}\right)^k\right]\right] \end{aligned} \tag{A.3}$$

Further simplifying the prefactor of the expression, we obtain:

$$6 \cdot \left(\frac{nn'}{n+n'}\right)^7 \cdot n \cdot n' \cdot (n'^2-1) \cdot (n'^2-4) \tag{A.4}$$

The remaining part of the expression, involving the sums, is then:

$$\begin{aligned} &\sum_{j=0}^{n-1}\left[\frac{((1-n)_j(7)_j)}{((2)_j j!)}\left(\frac{\frac{2}{n}}{\frac{1}{n'}+\frac{1}{n}}\right)^j\right. \\ &\quad \left. \times \sum_{k=0}^{n'-3}\left[\frac{((3-n')_k(7+j)_k)}{((6)_k k!)}\left(\frac{\frac{2}{n'}}{\frac{1}{n'}+\frac{1}{n}}\right)^k\right]\right] \end{aligned} \tag{A.5}$$

This formula provides an algebraic result for the integral of interest, providing therefore in principle an analytic result for the computation of the Love number k_2, and makes it possible to achieve in practice with Mathematica.

What is missing is the expression of the energy eigenvalues, which can be taken directly from "A quantum bound on compactness" since the energy eigenvalues for an hydrogen atom solution do not depend on angular quantum numbers:

$$\frac{\mathcal{E}_n}{M} \simeq -\frac{G_{\rm N}^2 M^4}{2\hbar^2 n^2} = -\frac{1}{2n^2}\left(\frac{M}{m_{\rm p}}\right)^4 = \frac{1}{2}\left(\frac{E_n^2}{M^2}-1\right) \tag{A.6}$$

We also have the condition:

$$0 \leq \frac{E_n^2}{M^2} \simeq 1 - \frac{1}{n^2}\left(\frac{M}{m_{\rm p}}\right)^4 \tag{A.7}$$

which gives:

$$n \geq N_M \simeq \left(\frac{M}{m_{\mathrm{p}}}\right)^2 \tag{A.8}$$

This gives then an idea of the order of magnitude of n, further for limitation of compute power we will assume a reasonably high value for n to make a computation for the k2 Love number instead of using directly the formula that relates it to the mass of the black hole.

Here is a computation of the k2 Love number for $n = 1000$ (assumed ground state), $n' = 1001, n' = 1002, n' = 1003$

using the formula:

$$k_2 = -\frac{3}{4R^5} \sum_{n_r} \frac{\left|\left\langle \Psi_0 | \hat{Q} | n_r, 2, 0 \right\rangle\right|^2}{|\Delta E_{1,n_r}|} \tag{A.9}$$

The sum will be performed by summing up the terms obtained by computing the argument of the sum for the respective n' values keeping n constant since considered ground state, an additional $\frac{1}{4\pi}$ was added to the multiplying constant to account for the integral of the angular part of the wavefunction.

In[48]:=
```
(*Constants*)n = 1000;
mp = Symbol["mp"]; (*Keeping mp,lp,and M as symbolic variables*)
lp = Symbol["lp"];
M = Symbol["M"];
R = Symbol["R"];  (*R is also a symbolic variable*)

(*Function to compute finalResult and deltaE for a given nPrime*)
computeResults[nPrime_] := Module[{const, firstPart, secondPart, finalResult, deltaE},
    (*Computation of const*)const = (mp^3 * lp / M^3) ^5 *
      (2 / nPrime) ^2 * (2 * M^3 / (mp^3 * lp)) ^3 * Sqrt[1 / (n^3 * nPrime^3) *
        ((n - 1) ! * (nPrime - 3) !) / (4 * n * nPrime * n ! * (nPrime + 2) !)];
    (*First Part of the Expression*)firstPart =
     6 * (n * nPrime / (n + nPrime)) ^7 * n * nPrime * (nPrime^2 - 1) * (nPrime^2 - 4);
    (*Second Part of the Expression*)
    secondPart = Sum[((Pochhammer[1 - n, j] * Pochhammer[7, j]) / (Pochhammer[2, j] * j !)) *
       ((2 / n) / (1 / nPrime + 1 / n)) ^j *
       Sum[((Pochhammer[3 - nPrime, k] * Pochhammer[7 + j, k]) / (Pochhammer[6, k] * k !)) *
         ((2 / nPrime) / (1 / nPrime + 1 / n)) ^k, {k, 0, nPrime - 3}], {j, 0, n - 1}];
    (*Final Result*)finalResult = Simplify[const * firstPart * secondPart];
    (*Calculation of deltaE*)
    deltaE = Abs[1 / (2 * n^2) - 1 / (2 * nPrime^2)] * (M^5 / mp^4);
    (*Return both finalResult and deltaE*){finalResult, deltaE}];

(*Computing results for nPrime=1001,1002,1003*)
{finalResult1, deltaE1} = N[computeResults[1001], 10];
{finalResult2, deltaE2} = N[computeResults[1002], 10];
{finalResult3, deltaE3} = N[computeResults[1003], 10];

(*Computing k2*)
k2 = -3 / (4 * R^5) * 1 / (4 * Pi) * ((finalResult1^2) / deltaE1 +
      (finalResult2^2) / deltaE2 + (finalResult3^2) / deltaE3);

(*Output k2 in a readable format*)
N[k2, 10]
```

Out[58]=

$$-\frac{4.77285410 \times 10^{31}\, lp^4\, mp^{16}}{M^{17}\, R^5}$$

Bibliography

[1] S. Weinberg, "Gravitation and Cosmology," John Wiley & Sons, 1972.

[2] R. D'Inverno, "Introducing Einstein's Relativity," Oxford University Press, 1992.

[3] E. Poisson, "A Relativist's Toolkit," Cambridge University Press, 2004.

[4] David J. Griffiths. *Introduction to Quantum Mechanics*. Available at: https://www.fisica.net/mecanica-quantica/Griffiths

[5] R. Casadio, "A quantum bound on the compactness," *Eur. Phys. J. C*, vol. 82, no. 10, 2022, doi:10.1140/epjc/s10052-021-09980-2.

[6] R. Brustein and Y. Sherf, "Classical Love number for quantum black holes," Physical Review D, vol. 105, no. 2, pp. 024044, 2022.

[7] R. Brustein and A. J. M. Medved, "Quantum hair of black holes out of equilibrium," Physical Review D, vol. 97, no. 4, pp. 044035, 2018.

[8] N. Gürlebeck, "No-hair theorem for black holes in astrophysical environments," Physical Review Letters, vol. 114, no. 15, pp. 151102, 2015.

[9] R. Brustein and Y. Sherf, "Quantum Love numbers," *Phys. Rev. D*, vol. 105, no. 2, pp. 024043, Jan. 2022, doi:10.1103/PhysRevD.105.024043. [Online]. Available: https://link.aps.org/doi/10.1103/PhysRevD.105.024043

[10] R. Brustein and A. J. M. Medved, "Black holes as collapsed polymers," Fortschritte der Physik (Progress of Physics), vol. 65, 1600114, 2017.

[11] N. Pinto-Neto and J. C. Fabris, "Quantum cosmology from the de Broglie–Bohm perspective," *Classical and Quantum Gravity*, vol. 30, no. 14, 143001, 2013, doi:10.1088/0264-9381/30/14/143001.

[12] N. Pinto-Neto, F. T. Falciano, R. Pereira, and E. S. Santini, "Wheeler-DeWitt quantization can solve the singularity problem," *Physical Review D*, vol. 86, no. 6, 063504, 2012, doi:10.1103/physrevd.86.063504.

[13] S. P. Kim, "Quantum potential and cosmological singularities," *Physics Letters A*, vol. 236, nos. 1–2, pp. 11–15, 1997, doi:10.1016/s0375-9601(97)00744-5.

[14] A. Vilenkin, "Approaches to quantum cosmology," *Physical Review D*, vol. 50, no. 4, pp. 2581–2594, 1994, doi:10.1103/physrevd.50.2581.